Comprehensive solutions to the Bloch equations and dynamical models for open two-level systems

Thomas E. Skinner

Phys. Rev. A **97**, 013815 — Published 12 January 2018

DOI: 10.1103/PhysRevA.97.013815

Comprehensive solutions of the Bloch equations and dynamical models of open two-level systems

Thomas E. Skinner*
Physics Department, Wright State University, Dayton, OH 45435
(Dated: December 11, 2017)

The Bloch equation and its variants constitute the fundamental dynamical model for arbitrary two-level systems. Many important processes, including those in more complicated systems, can be modeled and understood through the two-level approximation. It is therefore of widespread relevance, especially as it relates to understanding dissipative processes in current cutting-edge applications of quantum mechanics. Although the Bloch equation has been the subject of considerable analysis in the seventy years since its inception, there is still, perhaps surprisingly, significant work that can be done. This paper extends the scope of previous analyses. It provides a framework for more fully understanding the dynamics of dissipative two-level systems. A solution is derived that is compact, tractable, and completely general, in contrast to previous results. Any solution of the Bloch equation depends on three roots of a cubic polynomial that are crucial to the time dependence of the system. The roots are typically only sketched out qualitatively, with no indication of their dependence on the physical parameters of the problem. Degenerate roots, which modify the solutions, have been ignored altogether. Here, the roots are obtained explicitly in terms of a single real-valued root that is expressed as a simple function of the system parameters. For the conventional Bloch equation, a simple graphical representation of this root is presented that makes evident the explicit time dependence of the system for each point in the parameter space. Several intuitive, visual models of system dynamics are developed. A Euclidean coordinate system is identified in which any generalized Bloch equation is separable, i.e., the sum of commuting rotation and relaxation operators. The time evolution in this frame is simply a rotation followed by relaxation at modified rates that play a role similar to the standard longitudinal and transverse rates. The Bloch equation also describes a system of three coupled harmonic oscillators, providing additional perpsective on dissipative systems.

I. INTRODUCTION

The Bloch equation needs little formal introduction. It was proposed originally as a classical, phenomenological model for the dissipative dynamics observed in magnetic resonance [1]. However, its impact has been more widespread. It is applicable to general quantum two-level systems, which can be modeled [2] by the classical torque equations that underpin Bloch's analysis. As a result, the Bloch equation is employed in such diverse fields as quantum optics, spin models, atomic collisions, condensed matter, and quantum computing. Quantum control theory (see, for example, reviews in [3–5]) is another field for which the Bloch equation is increasingly relevant. Dissipation must be minimized to meet its ambitious goal of manipulating quantum systems to desired ends. Dissipative processes are of special topical interest for quantum computing, where coherence must be preserved.

The dynamics of this fundamental model for arbitrary, dissipative two-level quantum systems is therefore a topic of more than passing interest. One might well expect the landscape of the Bloch equation to be fully explored after seventy years. However, existing solutions [6–9] share some or all of the following limitations, leaving room for further development. They (i) are not sufficiently general to allow for arbitrary fields and relaxation models; (ii) depend on roots of a cubic polynomial that are not specified or related in any meaningful way to the physical parameters of the problem; (iii) divide by zero when the roots are degenerate, which occurs at values of the system parameters that are not specified; (iv) are cumbersome, conflated with the initial conditions and/or linked to tables of multiply nested variables with obscure connection to the physical parameters of the problem; (v) provide only a small measure of the physical insight that might be expected from an analytical solution.

In some respects, the complexity of the solutions make them only marginally better than a recipe for a numerical solution, which, in addition, is not completely general. As a separate issue, there are currently no intuitive visual models of system dynamics. Such models assist in the physical interpretation of the phenomena and often inspire further development in the field. Addressing the preceding matters might stimulate further advances towards understanding dissipative systems and controlling them for a desired outcome.

The paper proceeds as follows to address the aforementioned issues. A theoretical overview is provided in Sec. II. The intent is to give a fairly complete general understanding of the problem and the formal simplicity of the solution for arbitrary Bloch equation models. A benchmark for a more complete solution is defined at the outset by comparing previous Bloch equation solutions to the well-known solution for the damped harmonic oscillator. In addition, most previous treatments embed

* thomas.skinner@wright.edu

the initial conditions in the solution. The focus of the current solution is the propagator for the time evolution of the system. The initial conditions are disentangled from the dynamics. The physics does not depend on the initial conditions, so neither can the dynamics. Different initial conditions merely generate different trajectories for the system evolution, all driven by the same physics. The clarity provided in emphasizing the propagator contributed significant insight towards developing the intuitive dynamical models in the paper.

Section III is devoted to the explicit form of the propagator obtained formally in the previous section. A compact, complete solution to the Bloch equation is derived which is simpler than previous solutions, yet valid for arbitrary constant input parameters. The solutions are therefore applicable to more general but previously unsolved modified equations [10–22] proposed to address the failure of the original, conventional Bloch equation (OBE) to fully explain experimental data [23–25]. Moreover, the exact solutions are sufficiently simple that approximate limiting solutions [6–8] no longer provide any significant simplification. Conditions that result in division by zero in previous solutions are fully identified and addressed in the complete solution obtained here. A streamlined framework for obtaining and evaluating the roots of a cubic polynomial is developed that greatly facilitates the analysis. The roots required in the solution, i.e., system eigenvalues, are reduced to one real root obtained as a straightforward function of the physical parameters. Knowing this basic real root is sufficient to determine the others, simply and immediately. As is well known, the real parts of the roots are the dynamical relaxation rates, and the imaginary part, when it exists, is an oscillation frequency.

Section IV then focuses on the OBE. There, the dependence of the solutions on the physical parameters is characterized simply and in detail, neither of which have been done to date. The arithmetic difference between the spin-spin (transverse) and spin-lattice (longitudinal) relaxation rates provides a convenient and particularly useful frequency scale for representing system parameters in the analysis of the OBE. Quantitative bounds for oscillatory (underdamped) and non-oscillatory (critically damped and under damped) dynamics are derived. A simple graphical representation is obtained for the fundamental root as a function of the system parameters.

New models developed in Sec. V reveal the underlying simplicity of the dynamics. The Bloch equation is shown to represent a system of three mutually coupled damped harmonic oscillators. This model can also be cast in the form of frictionless coupled oscillators that are, nonetheless, damped. Both models provide new perspective on dissipative systems. The harmonic oscillator models are particular and explicit implementations of a more general result, namely, any quantum N-level system can be represented as a system of coupled harmonic oscillators [26, 27]. Although the dynamics are the same in either case, "there is a pleasure in recognizing old things from a new point of view" [28]. A different perspective can open the door to new insights. This treatment sets the stage for a simple vector model of Bloch equation dynamics. The trajectory of a system state in the model coordinates is simply a rotation followed by relaxation, which is easily visualized without recourse to the detailed analytical solution. A modified system of relaxation rates that emerges from the dynamics plays a role analogous to standard longitudinal and transverse relaxation effects. The modified rates result from the interaction/coupling between the fields and the phenomenological relaxation parameters of the particular Bloch model under consideration. Additionally, and incidentally, a method for finding eigenvectors emerges that does not appear to be widely known or utilized.

Details of the results and calculations in the text are deferred to appendices. The concluding appendix checks the solutions by applying them to a representative set of cases whose solutions can be straightforwardly obtained by other methods. Finally, the acronym OBE used henceforth also includes the optical Bloch equation (e.g., [29]).

II. THEORETICAL OVERVIEW

We first summarize the basic framework of the Bloch equation to recollect and define the fundamental parameters of the problem. The equation describes the dynamics of a magnetization $\boldsymbol{M}$ subjected to a static polarizing magnetic field $\boldsymbol{H}_0 = H_0\,\hat{\boldsymbol{z}}$ and a sinusoidal alternating field $2H_a \cos\omega_a t$ applied orthogonal to $\boldsymbol{H}_0$. For $H_a \ll H_0$, the equilibrium magnetization is not appreciably affected by the applied field and is therefore, to a good approximation, the time-independent value $\boldsymbol{M}_0 = \chi H_0\,\hat{\boldsymbol{z}}$ produced by the polarizing field.

One then considers a reference frame rotating about $\boldsymbol{H}_0$ at an angular frequency ω_a equal to the frequency of the applied field [30]. In this frame, the resulting effective field $\boldsymbol{H}_e$ is also time-independent. The evolution of the magnetization in this frame, neglecting dissipative effects, is simply a rotation about the field at the Larmor frequency $\boldsymbol{\omega}_e = -\gamma\boldsymbol{H}_e$ due to the torque $\gamma\boldsymbol{M}\times\boldsymbol{H}_e$ on $\boldsymbol{M}$, with $\boldsymbol{H}_e = (H_a\cos\phi, H_a\sin\phi, H_0 - \omega_a/\gamma)$. Here, γ is the gyromagnetic moment. An exact representation of the linearly polarized field $2H_a\cos\omega_a t$ also requires a counter rotating component. The rotating frame (NMR) or rotating wave (optics) approximation safely neglects this other frame when $H_a \ll H_0$, since then $\boldsymbol{H}_e \approx H_e\hat{\boldsymbol{z}}$ in the counter rotating frame and has negligible effect on the initial magnetization $M_0\hat{\boldsymbol{z}}$. The phase ϕ relative to the x-axis in the rotating frame is arbitrary in the context of a single applied field and has typically been set equal to zero in previous analyses of the Bloch equation. However, the relative phase is required for problems involving sequentially applied fields.

Relaxation rates R_i are then assigned to each component M_i to include dissipative processes. The torque can be written as a matrix-vector product [31], which, together with relaxation, gives the matrix

$$\Gamma = \begin{pmatrix} R_1 & \omega_3 & -\omega_2 \\ -\omega_3 & R_2 & \omega_1 \\ \omega_2 & -\omega_1 & R_3 \end{pmatrix} \tag{1}$$

comprised of the rates and the components of $\boldsymbol{\omega}_e$. In the original Bloch equation, the rates governing relaxation of the transverse magnetization components are equal, $R_1 = R_2$. More generally, modified Bloch equations can be considered in which the R_i are not equal, and, moreover, $\Gamma_{ij} \neq -\Gamma_{ji}$, as occurs for sufficiently strong fields and intensity-dependent damping[10–22]. Including the initial polarization M_0 or analogous equilibrium state relevant to a given application then gives a general Bloch equation of the form

$$\dot{\boldsymbol{M}}(t) + \Gamma \boldsymbol{M}(t) = \boldsymbol{M}_0 R_3. \tag{2}$$

The matrix Γ that drives the dynamics is completely general in what follows, within the context of time-independent fields and relaxation rates. Both $\boldsymbol{H}_e$ and $\boldsymbol{\omega}_e$ are referred to as fields in the OBE, since they are proportional. We further define the transverse field $\boldsymbol{\omega}_{12}$ as a component of the total field $\boldsymbol{\omega}_e$, with respective magnitudes (squared)

$$\begin{aligned} \omega_{12}^2 &= \omega_1^2 + \omega_2^2 \\ \omega_e^2 &= \omega_1^2 + \omega_2^2 + \omega_3^2. \end{aligned} \tag{3}$$

In the optical Bloch equation, the preceding fields become electric fields, magnetic moments are atomic dipole moments, ω_1 and ω_2 are proportional to the corresponding components of the applied electric field, and the resonance offset ω_3 is the difference between the atomic transition frequency and the frequency of the applied electric field.

A. An instructive analogy

The damped harmonic oscillator can be used to illustrate how the OBE solutions might be viewed as incomplete, notwithstanding the need for a more generally applicable solution. Consider first the original Torrey [6] solution. All other solutions to date are similar in content. As mentioned in the Introduction, any solution will depend on the roots of a cubic polynomial. The formula for these roots is well-known, if somewhat unwieldy, giving three roots of the form a and $b \pm i\,s$, in Torrey's notation, with a, b real and s either real or imaginary. No further details of the roots are given. The magnetization components, M_i, can then be obtained as

$$M_i(t) = A_i e^{-at} + e^{-bt}\left[B_i \cos st + \frac{C_i}{s}\sin st\right] + D_i. \tag{4}$$

The coefficients A_i, B_i, C_i, D_i are complicated functions of the physical parameters and the initial magnetization $M_i(0)$, typically listed in Tables in terms of multiply-nested variables. The D_i are the components of the steady-state magnetization. The roots are not specified further. In one instance [8], they are given in complicated form. Either way, none of the solutions provide any physical insight into the dependence of the decay and oscillation rates on the physical parameters of the problem. In addition, $s = 0$ results in doubly degenerate roots. The further condition $a = b$ gives a triple degeneracy. These degeneracies have not been fully noted or addressed.

Consider next the equation of motion for a damped harmonic oscillator under the influence of a constant force such as gravity. It can be written in the form

$$\ddot{x} + 2b\dot{x} + \omega_0^2 x = g. \tag{5}$$

The natural frequency of the oscillator is ω_0, with the velocity-dependent damping parameter b scaled by a factor of 2 to eliminate this factor from the solution. The standard approach tries a solution of the form e^{rt} for the $g = 0$ solution to the homogeneous equation, giving a quadratic polynomial in r. The two roots of a second-order polynomial are known to be of the form $r_\pm = -a \pm i\,s$, with a real and s either real or imaginary depending on the sign of the discriminant in the quadratic formula. The particular solution to Eq. (5) is $x(t) = g/\omega_0^2$, by inspection. With this minimal analysis, the solution obtained from $e^{r_\pm t}$ can be written in the form

$$x(t) = e^{-at}\left[A_1 \cos st + \frac{A_2}{s}\sin st\right] + D. \tag{6}$$

The steady-state $D = g/\omega_0^2$ is the constant displacement of the oscillator from the unperturbed, $g = 0$, equilibrium position. The coefficients A_i determined from the initial conditions are considerably simpler than the corresponding coefficients in Eq. (4).

Solutions for the Bloch equation proceed only this far. The damped oscillator is a much simpler system that is readily solved in more detail. The coordinates are typically shifted to define D as the new equilibrium position. The quadratic formula gives simple expressions for the roots and immediately shows that the decay rate will be the physical damping factor b. One easily proceeds further to obtain $s = (\omega_0^2 - b^2)^{1/2}$, giving (i) underdamped ($\omega_0^2 > b^2$), (ii) overdamped ($\omega_0^2 < b^2$), and (iii) critically damped ($\omega_0^2 = b^2$) solutions. The domain of applicability for each solution is clearly delineated as a function of the physical parameters b and ω_0. When $s = 0$, there is a single doubly degenerate root. The second linearly independent solution is te^{-bt}, giving

$$x_{s=0}(t) = e^{-bt}\left[A_1 + A_2 t\right] + D, \tag{7}$$

The constants A_i and D are the same as before, which is consistent with Eq. (6) in the limit $s \to 0$, using L'Hopital's rule. We will show in Sec. III that the same limiting process is valid for Eq. (4) by more formally finding the linearly independent solutions in the case of degenerate roots.

The failure of the OBE solutions to match the completeness of the damped oscillator solution is not particularly surprising. The OBE appears to have five independent parameters (the elements of Γ in Eq. (1) with $R_1 = R_2$). Analysis of the system is far more complex, appearing perhaps too complex for a more illuminating result. However, a simpler realization of cubic roots developed here and more detailed investigation of the roots resulting from the OBE shows only three independent parameters, two of which can be scaled in terms of the third to give a two-parameter problem similar to the damped oscillator.

One might also be intrigued by the similarity of the solutions for the damped oscillator and the Bloch equation. This correspondence is not accidental, and will be pursued further in Sec. V, where the Bloch equation is modeled exactly by a system of three coupled, damped harmonic oscillators. In addition, the dynamics of a single damped oscillator is known to be simple in the $(x, \dot{x})$ phase plane (see, for example, Marion [32]). The underdamped trajectory is related to a logarithmic spiral, while the overdamped trajectory traces out a non-oscillatory asymptotic decay to zero. The analogous visual model for Bloch equation dynamics is developed in Sec. V C.

But first, we extend the Bloch equation solution to arbitrary (constant) parameter models. The new solution is simpler and more convenient to use than existing OBE solutions, which, in addition, are problematic for particular configurations of the parameter space.

B. Bloch equation solution

A standard approach to solving a system of inhomogeneous equations such as Eq. (2) is to transform it to a homogeneous form [33] by appending the inhomogeneous term $\boldsymbol{M}_0 R_3$ as a column to the right of Γ and then adding a correspondingly expanded row of zeros at the bottom. The vector $\boldsymbol{M}$ would then be augmented by including a last element equal to one. Increasing the dimensionality of the problem in this way can be rather trivially avoided by defining

$$\mathcal{M}(t) \equiv \boldsymbol{M}(t) - \boldsymbol{M}_\infty, \tag{8}$$

where $\boldsymbol{M}_\infty = \Gamma^{-1}\boldsymbol{M}_0 R_3$. This is the same shift in coordinates to the equilibrium (steady-state) position that is commonly employed for the harmonic oscillator example of Eq. (5). There, the result of a constant force is a shifted equilibrium position $x \to (\omega_0^2)^{-1} g$, which gives a homogeneous equation in the shifted coordinates. Since $\boldsymbol{M}_\infty$ is constant, we have

$$\dot{\mathcal{M}}(t) = -\Gamma\,\mathcal{M}(t) \tag{9}$$

with solution

$$\begin{aligned}
\mathcal{M}(t) &= e^{-\Gamma t}\mathcal{M}(0) && \text{(10a)}\\
\boldsymbol{M}(t) &= e^{-\Gamma t}\left[\boldsymbol{M}(0) - \boldsymbol{M}_\infty\right] + \boldsymbol{M}_\infty && \text{(10b)}\\
&= e^{-\Gamma t}\boldsymbol{M}(0) + (1 - e^{-\Gamma t})\boldsymbol{M}_\infty && \text{(10c)}
\end{aligned}$$

as a function of the steady-state $\boldsymbol{M}_\infty$ and transient $\boldsymbol{M}(0)$ responses. The crux of the problem, then, is a solution for the propagator $e^{-\Gamma t}$. Framing the problem most generally to include arbitrary Γ might be expected to complicate the solution compared to previous treatments. However, emphasizing the solution for the propagator results in a compact and relatively simple solution.

C. The propagator $e^{-\Gamma t}$

There are numerous methods, both analytical and numerical, for calculating a matrix exponential [Moler and van Loan [34] and references therein]. The Laplace transform will be employed here, both for historical reasons (it has been utilized in previous Bloch equation solutions) and because most of the other analytical methods can be derived from it. This is a topic worth developing in its own right that is beyond the scope of the present article.

The Laplace transform $\mathcal{L}$ of e^{-at} is equal to $(s+a)^{-1}$ for constant a. The matrix exponential $e^{-\Gamma t}$ for constant Γ is then the inverse Laplace transform $\mathcal{L}^{-1}\left[\,(s\mathbb{1}+\Gamma)^{-1}\,\right]$, where $\mathbb{1}$ is the identity element. The inverse Laplace transform of a function $f(s)$ can be written in terms of the Bromwich integral as [see, for example, Arfken [35]]

$$\begin{aligned}
\mathcal{L}^{-1}[f(s)] &= \frac{1}{2\pi i}\int_{\gamma - i\infty}^{\gamma + i\infty} f(s)e^{st}\,ds\\
&= F(t),
\end{aligned} \tag{11}$$

where the real constant γ is chosen such that $\mathrm{Re}\,(s) < \gamma$ for all singularities of $f(s)$. Closing the contour by an infinite semicircle in the left half plane ensures convergence of the integral for $t > 0$. The desired $F(t)$ is then the sum of the residues of the integrand.

For $f(s) = (s\mathbb{1}+\Gamma)^{-1}$, recall the textbook theorem for the inverse of a matrix A, with terms defined as follows:

(i) $A(i|j)$ is the matrix obtained by deleting row i and column j of A.

(ii) The cofactor of A_{ij} is $C_{ij} = (-1)^{i+j}$ times the determinant $\det A(i|j)$.

(iii) The adjugate of A is the matrix $(\mathrm{adj}\,A)_{ij} = C_{ji}$, i.e., the transpose of the cofactor matrix for A, which is the same as the cofactors of A transpose.

Then

$$A^{-1} = \mathrm{adj}\,A/\det A. \tag{12}$$

The matrix

$$A(s) = s\mathbb{1} + \Gamma \tag{13}$$

gives

$$\det\, A(s) = p(s), \tag{14}$$

where $p(s)$ is the characteristic polynomial of $(-\Gamma)$.

The desired solution for $F(t) = e^{-\Gamma t}$ is then the sum of the residues of the integrand in Eq. (11), with $f(s) \to (s\mathbb{1} + \Gamma)^{-1} = \operatorname{adj} A(s)/p\,(s)$ giving

$$e^{-\Gamma t} = \sum_{\text{res}} \frac{\operatorname{adj} A(s)}{p\,(s)}\, e^{st} \tag{15}$$

for any Γ. The poles clearly occur at the roots of $p(s)$, i.e., the eigenvalues of $-\Gamma$. The propagator is therefore constructed fairly simply from Γ and its eigenvalues.

Recall for reference in what follows that for a function $g(s)$ with a pole of order k at $s = s_0$, the coefficient of $(s - s_0)^{-1}$ in the Laurent series expansion of $g(s)$ about $s = s_0$, i.e., the residue at s_0, is

$$\text{res}\,(s_0) = \frac{1}{(k-1)\,!} \lim_{s \to s_0} \frac{d^{\,k-1}}{ds^{k-1}} \left[\,(s - s_0)^k\, g(s)\,\right] \tag{16}$$

III. SOLUTIONS FOR THE PROPAGATOR

The results obtained so far provide the basis for a complete, compact, general solution of the Bloch equation, developed in detail, next. The solution for the matrix exponential $e^{-\Gamma t}$ is valid for any time-independent 3×3 matrix Γ. Degenerate roots of the characteristic polynomial, which give rise to division by zero in previous solutions, are fully addressed in the form of the solution given in Eq. (15).

A. Roots of the characteristic polynomial

The solution for $e^{-\Gamma\, t}$ given in Eq. (15) requires the roots of $p(s)$ in Eq. (14). The resulting third degree polynomial is

$$p\,(s) = c_{\,0} + c_1 s + c_2 s^2 + s^3 \tag{17}$$

with coefficients

$$\begin{aligned}
c_{\,0} \;&=\; \prod_j R_j - \frac{1}{2} \sum_{j \neq k \neq l} R_j\, \Gamma_{kl} \Gamma_{lk} + \\
&\qquad \Gamma_{12}\Gamma_{23}\Gamma_{31} + \Gamma_{21}\Gamma_{32}\Gamma_{13} \\
&\overset{\text{OBE}}{\longrightarrow} \prod_j R_j + \sum_j R_j\, \omega_j^2 \\
c_1 \;&=\; -\sum_{\substack{j \neq k \\ j<k}} \Gamma_{jk}\Gamma_{kj} + \sum_{j<k} R_j R_k \\
&\overset{\text{OBE}}{\longrightarrow} \omega_e^2 + R_1 R_2 + R_1 R_3 + R_2 R_3 \\
&= \omega_e^2 + \sum_{j<k} R_j R_k \\
c_2 \;&=\; \sum_i R_i\,.
\end{aligned} \tag{18}$$

As is well known, the substitution $s = z - c_2/3$ reduces Eq. (17) to the standard canonical form

$$\begin{aligned} p\,(z - c_2/3) &= z^3 + \tilde{c}_1 z + \tilde{c}_0 \\ &= q\,(z), \end{aligned} \tag{19}$$

where

$$\begin{aligned} \tilde{c}_0 &= 2\left(\frac{c_2}{3}\right)^3 - c_1\left(\frac{c_2}{3}\right) + c_0 \\ \tilde{c}_1 &= c_1 - c_2^2/3 \end{aligned} \tag{20}$$

Solutions for the roots z_i are then available as functions of $\tilde{c}_0$ and $\tilde{c}_1$ from standard formulas. However, these formulas are relatively complicated functions of the polynomial coefficients (and hence, the physical parameters in the Bloch equation), which hinders physical insight. In Appendix C, simpler expressions are derived for the roots that reduce their complexity compared to previous treatments. The fundamental results are summarized below.

Any polynomial with real coefficients has at least one real root, assigned here to z_1. The solutions can then be consolidated in a convenient form that does not appear to have been employed before. The other two roots are written as a function of z_1,

$$\begin{aligned} z_{2,3} &\equiv z_\pm \\ &= -\frac{1}{2} z_1 \,\pm\, i\,\varpi\,, \end{aligned} \tag{21}$$

in terms of a discriminant

$$\varpi^2 = 3\big[(z_1/2)^2 + \tilde{c}_1/3\big], \tag{22}$$

which will be positive, negative, or zero depending on the value of z_1, the sign of $\tilde{c}_1$, and their relative magnitudes.

The roots are further characterized here in terms of the positive parameter

$$\gamma = \frac{|\tilde{c}_0/2|}{|\tilde{c}_1/3|^{3/2}}, \tag{23}$$

leading to the following delineation of the roots:

(i) $\tilde{c}_1 > 0$, or, $\tilde{c}_1 < 0$ and $\gamma > 1$

3 distinct roots (1 real, 2 complex conjugate)

(ii) $\tilde{c}_1 < 0$ and $\gamma < 1$

3 distinct real roots

(iii) $\tilde{c}_1 < 0$ and $\gamma = 1$

2-fold degenerate roots $z_+ = z_- = -\frac{1}{2} z_1$

(iv) $\tilde{c}_0 = 0 = \tilde{c}_1$

3-fold degenerate roots $z_i = 0$

The physical parameters that define these effective domains for the roots are derived for the OBE in Sec. IV.

In addition, we will find that the sign of $\tilde{c}_0$ determines the sign of z_1. Thus, in all cases, the set of three roots for a given $\tilde{c}_0 < 0$ is equal and opposite to the set obtained for parameters that flip the sign of $\tilde{c}_0$. The case $\tilde{c}_0 = 0$ (i.e., $\gamma = 0$) reduces simply to $z_1 \sim \mathrm{sgn}(0) = 0$. From Eqs. (21) and (22), there are then two additional real or imaginary roots depending on the sign of ϖ^2.

The roots of $p\,(s = z - c_2/3)$ are then

$$s_i = z_i - c_2/3\,, \tag{24}$$

where, referring to Eq. (18),

$$\frac{c_2}{3} = \frac{1}{3}\sum_i R_i \equiv \bar{R} \tag{25}$$

is the average of the relaxation rates.

B. Cayley-Hamilton Theorem

The expression for $e^{-\Gamma t}$ in Eq. (15) also depends on $\mathrm{adj}\,A(s)$. The elements of $\mathrm{adj}\,A(s)$, are simple (2×2) determinants, giving

$$\mathrm{adj}\,A(s) = A_0 + A_1\,s + \mathbb{1}\,s^2, \tag{26}$$

a polynomial in s with coefficient matrices

$$A_0 = c_1\mathbb{1} - c_2\,\Gamma + \Gamma^2, \qquad A_1 = c_2\mathbb{1} - \Gamma, \tag{27}$$

as shown in Appendix A. The result can be readily generalized to higher dimensional matrices, but this exceeds the scope of the present work.

Substituting Eq. (27) into Eq. (26) and rearranging terms gives

$$\begin{aligned}\mathrm{adj}\,A(s) &= (c_1 + c_2 s + s^2)\mathbb{1} + (c_2 + s)(-\Gamma) + \Gamma^2\\ &= \sum_{j=0}^{2} p_j(s)\,(-\Gamma)^j,\end{aligned} \tag{28}$$

which defines the polynomial coefficients $p_j(s)$. Further defining

$$a_j(t) = \sum_{\mathrm{res}} \frac{p_j(s)}{p\,(s)}\,e^{st}, \qquad j = 0, 1, 2 \tag{29}$$

then yields a solution for the propagator in the form

$$\begin{aligned}e^{-\Gamma t} &= \sum_{j=0}^{2} a_j(t)(-\Gamma)^j\\ &= (\mathbb{1}, -\Gamma, \Gamma)\begin{bmatrix} a_0(t)\\ a_1(t)\\ a_2(t)\end{bmatrix}\end{aligned} \tag{30}$$

where the sum has been expressed as multiplication of a row and column matrix. We therefore have a concise implementation of the Cayley-Hamilton theorem, which states that every square matrix is a solution to its characteristic equation. As a consequence, $-\Gamma$ is a solution of Eq. (17). One can solve for Γ^3, and subsequently for all higher powers of Γ, in terms of the set $\{\mathbb{1}, -\Gamma, \Gamma^2\}$. The series expansion of $e^{-\Gamma\,t}$ can then be expressed in terms of the same set, as above.

The coefficient polynomial $p_j(s)$ multiplying $(-\Gamma)^j$ can be defined recursively as

$$\begin{aligned}p_{-1}(s) &\equiv p(s)\\ p_j(s) &= \frac{p_{j-1}(s) - c_j}{s},\end{aligned} \tag{31}$$

i.e., $p_j(s)$ is obtained by dividing $p(s)$ by s^{j+1} and removing all terms with s in the denominator from the result. The matrix exponential given in Eq. (30) is then readily generalized to matrices of arbitrary dimension.

C. A convenient matrix partitioning

We first seek to avoid transforming the characteristic polynomial to canonical form, solving for these roots, then transforming back to obtain the roots of the original polynomial. The result of this endeavor leads to additional simplifications in what follows.

Partition Γ as the sum of commuting matrices

$$\begin{aligned}\Gamma &= \mathcal{R} + \Gamma_{\mathrm{p}}\\ &= \bar{R}\,\mathbb{1} + \begin{pmatrix} R_{1\mathrm{p}} & \Gamma_{12} & \Gamma_{13}\\ \Gamma_{21} & R_{2\mathrm{p}} & \Gamma_{23}\\ \Gamma_{31} & \Gamma_{32} & R_{3\mathrm{p}}\end{pmatrix},\end{aligned} \tag{32}$$

where, as before, $\bar{R}$ is the average of the R_i as in Eq. (25), and the diagonal elements of Γ_{p} are

$$\begin{aligned}R_{i\mathrm{p}} &= R_i - \bar{R}\\ &= \frac{2}{3}R_i - \frac{1}{3}\sum_{j\neq i} R_j.\end{aligned} \tag{33}$$

The coefficients $c_{i\mathrm{p}}$ in the characteristic polynomial for $-\Gamma_{\mathrm{p}}$ are obtained from Eq. (18) with $R_i \to R_{i\mathrm{p}}$. Then, $c_{2\mathrm{p}} = \sum_i R_{i\mathrm{p}} = 0$, and $p(s)$ is in the standard canonical form $q(z)$ of Eq. (19), with coefficients $c_{i\mathrm{p}} \equiv \tilde{c}_i$. We then have

$$e^{-\Gamma t} = e^{-\bar{R}\,t} e^{-\Gamma_{\mathrm{p}}\,t}. \tag{34}$$

The focus henceforth will be the solution for $e^{-\Gamma_{\mathrm{p}}\,t}$ using Eq. (30), with the obvious substitutions $\Gamma \to \Gamma_{\mathrm{p}}$, $p_j \to q_j$, and $c_j \to \tilde{c}_j$. The roots $s_i = z_i$ are given in Eq. (C6).

D. Simple pole solution

When the roots z_i of $q\,(z)$ are distinct, the residues are due to simple first-order poles, z_n. Factor $q\,(z)$ as $\prod_i (z - z_i)$. Then $(z - z_n)/q\,(z) = \prod_{i\neq n}(z - z_i)$, as needed to evaluate the residue at z_n. The derivative $q'(z) = \sum_j \prod_{i\neq j}(z - z_i)$ evaluated at z_n is also equal to $\prod_{i\neq n}(z_n - z_i)$, since the other terms in the sum vanish at $z = z_n$. Summing the residues in Eq. (29) at the three roots gives

$$a_j(t) = \sum_{i=1}^{3} \frac{q_j((z_i)}{q'(z_i)} e^{\,z_i t} \tag{35}$$

The derivative of the characteristic polynomial can be calculated from either the factored form involving the roots or the polynomial form in Eq. (17). Each provides information that might be useful for different applications. The matrix exponential $e^{-\Gamma_{\rm p} t}$ can then be written compactly as matrix multiplication in the form

$$\begin{aligned} e^{-\Gamma_{\rm p} t} &= (\mathbb{1}, -\Gamma_{\rm p}, \Gamma_{\rm p}^2\,) \begin{bmatrix} a_0(t) \\ a_1(t) \\ a_2(t) \end{bmatrix} \\ &= (\mathbb{1}, -\Gamma_{\rm p}, \Gamma_{\rm p}^2\,)\,[\,W_1(z_1)\,\boldsymbol{u}_1(t)\,]\,, \\ W_1(z_1) &= \begin{pmatrix} z_1^2 + \tilde{c}_1 & z_2^2 + \tilde{c}_1 & z_3^2 + \tilde{c}_1 \\ z_1 & z_2 & z_3 \\ 1 & 1 & 1 \end{pmatrix} \\ \boldsymbol{u}_1(t) &= \begin{pmatrix} e^{z_1 t}/q'(z_1) \\ e^{z_2 t}/q'(z_2) \\ e^{z_2 t}/q'(z_2) \end{pmatrix}\,. \end{aligned} \tag{36}$$

For parameter values

(i) $\tilde{c}_1 > 0$ or $\tilde{c}_1 < 0$ and $\gamma > 1$,

ϖ is real from Eqs. (C6a) and (C6b), so two of the roots are complex conjugates. Although Eq. (36)) is the most straightforward form of the solution and readily used in numerical calculations, individual terms are complex. A more transparently real-valued expression is obtained by performing the sum in Eq. (35) after rationalizing complex denominators and writing the roots $z_{2,3}$ in terms of z_1 using Eqs. (21) and (22), as detailed in Appendix D. The result is of the form in Eq. (36) with

$$\begin{aligned} W_1(z_1) &\to \frac{1}{3z_1^2 + \tilde{c}_1} \begin{pmatrix} z_1^2 & 2z_1^2 & -\tilde{c}_1 z_1 \\ z_1 & -z_1 & \frac{3}{2}z_1^2 + \tilde{c}_1 \\ 1 & -1 & -\frac{3}{2}z_1 \end{pmatrix} \\ \boldsymbol{u}_1(t) &\to \begin{pmatrix} e^{z_1 t} \\ e^{-z_1 t/2}\,\cos\varpi t \\ e^{-z_1 t/2}\,\dfrac{\sin\varpi t}{\varpi} \end{pmatrix}\,. \end{aligned} \tag{37}$$

The coefficient $\tilde{c}_1$ can be found in terms of the roots z_i upon expanding the factored form for $q(z)$ to obtain $\tilde{c}_1 = z_1 z_2 + z_1 z_3 + z_2 z_3$. The solution for the matrix exponential is thus separable into a term that depends directly on the physical parameters of the problem through Γ_p, a term that depends on the roots z_i, and a term that gives the time dependence, which in turn is solely a function of the roots.

For the case

(ii) $\tilde{c}_1 < 0$ and $\gamma < 1$,

ϖ is imaginary, as given by Eq. (C6c), so there are three real roots. There is no oscillatory behavior in the straightforward result given in Eq. (36). The solution can be written alternatively in terms of $\mu = |\varpi|$ using Eq. (37), with $\varpi = i\mu$ giving $\cos\varpi\,t \to \cosh\mu\,t$ and $\sin\varpi\,t/\varpi \to \sinh\mu\,t/\mu$.

E. Second-order pole solution

For

(iii) $\tilde{c}_1 < 0$ and $\gamma = 1$,

we have $\varpi = 0$ in either Eq. (C6b) or Eq. (C6c), which implies $\tilde{c}_1 \to -3(z_1/2)^2$ according to Eq. (22). Then two of the three real roots are equal, giving a doubly degenerate root $z_2 = z_3 = -z_1/2$. The characteristic polynomial $q\,(z) \to (z - z_1)(z - z_2)^2$. The contribution from the first-order pole at z_1 is obtained as before, i.e., the first column of $W_1(z_1)$ and the first element of $u_1(t)$ in Eq. (37) remain the same. The residue at z_2 is calculated in Appendix D, leading to a solution

$$\begin{aligned} e^{-\Gamma_{\rm p} t} &= (\mathbb{1}, -\Gamma_{\rm p},\, \Gamma_{\rm p}^2\,)\,[\,W_2(z_1)\,\boldsymbol{u}_2(t)\,]\,, \\ W_2(z_1) &= \begin{pmatrix} \dfrac{1}{9} & \dfrac{8}{9} & \dfrac{1}{3}z_1 \\[2ex] \dfrac{4}{9}z_1^{-1} & -\dfrac{4}{9}z_1^{-1} & \dfrac{1}{3} \\[2ex] \dfrac{4}{9}z_1^{-2} & -\dfrac{4}{9}z_1^{-2} & -\dfrac{2}{3}z_1^{-1} \end{pmatrix} \\ \boldsymbol{u}_2(t) &= \begin{pmatrix} e^{z_1 t} \\ e^{-z_1 t/2} \\ t e^{-z_1 t/2} \end{pmatrix}\,. \end{aligned} \tag{38}$$

There is thus a term linear in the time, t. Note that Eq. (38) is also the limit of Eq. (37) as $\varpi \to 0$ and $\tilde{c}_1 \to -3(z_1/2)^2$, providing an independent verification of the simple-pole result. One could anticipate on physical grounds that the separate solutions obtained for distinct and degenerate roots should be continuous in this limit. However, it is an assumption that is verified by properly calculating the solution for a second-order pole.

F. Third-order pole solution

The case

(iv) $\tilde{c}_0 = 0 = \tilde{c}_1$

gives a triply degenerate, real root $z_1 = 0$ for $q\,(z) \to z^3$. The $a_j(t)$ are evaluated in Appendix D, giving $a_0(t) = 1$, $a_1(t) = t$, and $a_2(t) = t^2/2$, so that

$$e^{-\Gamma_{\rm p} t} = \mathbb{1} - \Gamma_{\rm p}\,t + \tfrac{1}{2}\Gamma_{\rm p}^2\,t^2\,. \tag{39}$$

There is now a term that is quadratic in the time. The same result is obtained from Eq. (38) in the limit $z_1 \to 0$ upon series expansion of the exponential terms. In addition, the Cayley-Hamilton theorem is simple to apply directly in this case, since $q(-\Gamma_\mathrm{p}) = -\Gamma_\mathrm{p}^3 = 0$. The series expansion of $e^{-\Gamma_\mathrm{p} t}$ is therefore truncated, giving the Eq. (39) result directly and verifying the self-consistency of the solutions.

G. Steady state solution

The steady state response $\boldsymbol{M}_\infty$ defined in Eq. (10) is equal to $\Gamma^{-1}\boldsymbol{M}_0 R_3$, with $\Gamma^{-1} = \mathrm{adj}\,\Gamma/\det(\Gamma)$. The dependence on adj Γ is only in the third column, since $\boldsymbol{M}_0$ is along $\hat{\boldsymbol{z}}$, with $\det(\Gamma) = p(0)$ given by c_0 in Eq. (18). Then

$$\boldsymbol{M}_\infty = \frac{M_0 R_3}{c_0}\begin{bmatrix} \Gamma_{12}\Gamma_{23} - \Gamma_{13}R_2 \\ \Gamma_{13}\Gamma_{21} - \Gamma_{23}R_1 \\ -\Gamma_{12}\Gamma_{21} + R_1R_2 \end{bmatrix} \tag{40a}$$

$$\xrightarrow{\text{OBE}} \frac{\chi H_0 R_3}{R_1R_2R_3\left(1 + \displaystyle\sum_{i\neq j\neq k}\frac{\omega_i^2}{R_jR_k}\right)}\begin{bmatrix} \omega_1\omega_3 + \omega_2 R_2 \\ \omega_2\omega_3 - \omega_1 R_1 \\ \omega_3^2 + R_1R_2 \end{bmatrix}. \tag{40b}$$

Letting $R_1 = R_2 = 1/T_2$ and $R_3 = 1/T_1$ gives

$$\boldsymbol{M}_\infty \xrightarrow{\text{OBE}} \frac{\chi H_0}{1 + T_1T_2\,\omega_{12}^2 + T_2^2\,\omega_3^2}\begin{bmatrix} T_2\,(\omega_1\omega_3T_2 + \omega_2) \\ T_2\,(\omega_2\omega_3T_2 - \omega_1) \\ 1 + T_2^2\,\omega_3^2 \end{bmatrix}, \tag{41}$$

which reduces to Bloch's result [1], obtained for $\omega_2 = 0$.

For the specific case of the OBE on resonance ($\omega_3 = 0$), Lapert *et al.* [36] give a geometric interpretation of the steady state as points on the surface of an ellipsoid satisfying the equation

$$\frac{M_x^2 + M_y^2}{T_2} + \frac{(M_z - 1/2)^2}{T_1} = \frac{1}{4T_1}. \tag{42}$$

We note here that the result is more general. The components of $\boldsymbol{M}_\infty$ in Eq. (41) for the off resonance OBE also satisfy Eq. (42), as does the result in Eq. (40a) when $\Gamma_{ji} = -\Gamma_{ij}$ and $R_1 = R_2$. The magic plane defined in that work is also independent of resonance offset, ω_3.

IV. THE CONVENTIONAL BLOCH EQUATION

The solutions can be further simplified when applied to the specific parameters of the OBE. The approach taken here allows us to delve deeper than previous analyses to obtain additional insight into the nature of the solutions and the constraints that determine root multiplicities. Substituting $R_1 = R_2$ gives the rates R_{ip} in Γ_p of Eq. (32). Define

$$R_\delta = \frac{R_2 - R_3}{3} \geq 0, \tag{43}$$

since the transverse relaxation rate R_2 is greater than or equal to the longitudinal rate R_3 in physical systems. Then

$$R_{1p} = R_{2p} = R_\delta, \qquad R_{3p} = -2R_\delta. \tag{44}$$

The coefficients of the characteristic polynomial for $-\Gamma_\mathrm{p}$ then simplify to

$$\begin{aligned} \tilde{c}_0 &= R_\delta\left[\,\omega_e^2 - 2\,R_\delta^2 - 3\,\omega_3^2\,\right] \\ \tilde{c}_1 &= \omega_e^2 - 3R_\delta^2\,. \end{aligned} \tag{45}$$

The rate R_δ provides a convenient and simplifying frequency scale for characterizing the solutions in the sections which follow.

A. Criteria for the existence of degenerate roots

The resulting simpler form for the polynomial coefficients makes possible a straightforward analysis of the conditions for which there are degeneracies in the roots. As discussed in section III A, there is a two-fold degeneracy in the roots for $\gamma = 1$. This is equivalent, using Eq. (23) for γ, to

$$\begin{aligned} D(\tilde{c}_0, \tilde{c}_1) &= (\tilde{c}_0/2)^2 + (\tilde{c}_1/3)^3 \\ &= 0. \end{aligned} \tag{46}$$

The trivial solution $\tilde{c}_1 = 0 = \tilde{c}_0$ gives a three-fold degenerate root $z_i = 0$.

Details are deferred to Appendix E, where the existence of degenerate roots is characterized in terms of

$$\omega_3^2 = \lambda_3 R_\delta^2/3 \qquad \text{and} \qquad \omega_{12}^2 = \lambda_{12}R_\delta^2/3. \tag{47}$$

For each ω_3 defined by the range $0 \leq \lambda_3 \leq 1$, one finds two solutions for λ_{12} that satisfy $D(\tilde{c}_0, \tilde{c}_1) = 0$ and give real values for ω_{12}. Thus, for each $\omega_3 \in [\,0, R_\delta^2/3\,]$, there are two values of ω_{12} that produce degeneracies in the roots z_i. The two solutions for λ_{12} can be expressed concisely in the form

$$\begin{aligned} \lambda_{12,i} &= \eta_i - \lambda_3 + \tfrac{9}{4} \qquad\qquad i = 1,2 \\ \eta_i &= \tfrac{9}{2}\sqrt{8\lambda_3 + 1}\,\sin\vartheta_i \\ \vartheta_1 &= \mathrm{sgn}(\lambda_3 - \lambda_b)\,\tfrac{1}{3}\sin^{-1}\frac{|8\lambda_3^2 + 20\lambda_3 - 1|}{(8\lambda_3 + 1)^{3/2}} \\ \vartheta_2 &= \pi/3 - \vartheta_1 \end{aligned} \tag{48}$$

for $\lambda_b = \frac{3}{4}(\sqrt{3} - \frac{5}{3})$. The solutions converge at $\lambda_3 = 1$ to $\eta_1 = \eta_2 = 27/4$, giving $\omega_{12}^2 = 8(R_\delta^2/3)$. Then $\tilde{c}_1 = 0 = \tilde{c}_0$ from Eq. (45), giving the three-fold degenerate root $z_i = 0$ of Eq. (19) mentioned above.

The following simple and explicit criteria characterize the poles in Eqs. (15) and (29):

(i) $\omega_3^2 > R_\delta^2/3$

There is no real-valued solution for ω_{12}^2 such that $\gamma = 1$, i.e., $D(\tilde{c}_0, \tilde{c}_1) = 0$, and, hence, the roots z_i are distinct.

(ii) $\omega_3^2 < R_\delta^2/3$

There are two different real-valued solutions for ω_{12}^2 as a function of λ_3 that each give a two-fold degeneracy in the roots z_i, requiring the second-order pole solution of Eq. (38). Otherwise, the roots are distinct.

(iii) $\omega_3^2 = R_\delta^2/3$

gives $\omega_{12}^2 = 8(R_\delta^2/3)$ for $\lambda_3 = 1$, resulting in a three-fold degenerate root $z_i = 0$ which requires the third-order pole solution of Eq. (39).

B. Characterization of the damping

Solutions for the roots z_i are characterized according to whether the discriminant ϖ^2 of Eq. (22) is positive, negative, or zero, and can be described, respectively, as underdamped, overdamped, or critically damped, analogous to a damped harmonic oscillator.

The solution for the propagator in the case of degenerate roots ($\gamma = 1$) has a term linear in time, characteristic of a critically damped harmonic oscillator. For a three-fold degeneracy in the roots, there is an additional term that is quadratic in the time. The values of ω_3^2 that allow degeneracies are restricted to the narrow range parameterized according to $0 \le \lambda_3 \le 1$, as discussed in the previous section. The two solutions $\omega_{12,1}^2$ and $\omega_{12,2}^2$ for each ω_3^2, as determined from Eqs. (47) and (48), are the solid curves plotted in Fig. 1.

Using the same scaling of ω_3 and ω_{12} as in Eq. (47), we also have

$$\begin{aligned}
\tilde{c}_0(\lambda_{12}, \lambda_3) &= (\lambda_{12} - 2\lambda_3 - 6)\, R_\delta^3/3 \\
\tilde{c}_1(\lambda_{12}, \lambda_3) &= (\lambda_{12} + \lambda_3 - 9)\, R_\delta^2/3 \\
\gamma(\lambda_{12}, \lambda_3) &= \frac{9}{2}\, \frac{|\lambda_{12} - 2\lambda_3 - 6|}{|\lambda_{12} + \lambda_3 - 9|^{3/2}}
\end{aligned} \tag{49}$$

Solutions in the range $\omega_{12,1}^2 < \omega_{12}^2 < \omega_{12,2}^2$ bounded by the critical damping parameters give $\tilde{c}_1 < 0$ and $\gamma < 1$, resulting in three distinct real roots and overdamped evolution. The range of bounding values is fairly narrow, becoming increasingly so with increasing λ_3 and converging to a single value $\omega_{12}^2 = 8R_\delta^2/3$ as $\lambda_3 \to 1$, as shown in the figure.

Underdamped, oscillatory solutions are obtained for all other field values, either $\omega_3^2 > R_\delta^2/3$ (i.e., $\lambda_3 > 1$) or $\omega_{12}^2 \ge \omega_{12,1}^2$ and $\omega_{12}^2 \le \omega_{12,2}^2$ for $\lambda_3 \le 1$.

C. Characterization of the roots

The solution to the Bloch equation has a relatively simple form and can be expressed in terms of a single root, z_1, of the characteristic polynomial for $-\Gamma_p$. Although the solutions for z_1 have also been expressed in relatively simple functional form, these forms provide little physical insight. It remains to shed some light on the dependence of this root on the field $\boldsymbol{\omega}_e$ and the relaxation rates.

1. Physical limits of the roots

Since the roots z_i are functions of $\tilde{c}_0, \tilde{c}_1$ and γ, they also scale as R_δ. The associated decay rates are $\mathrm{Re}(s_i) = \mathrm{Re}(z_i) - \bar{R}$, from Eq. (24). Defining

$$\lambda_z = \mathrm{Re}(z_i)/R_\delta. \tag{50}$$

and using Eq. (43) for R_δ gives the decay rates

$$\begin{aligned}
\mathrm{Re}(s_i) &= \lambda_z R_\delta - \bar{R} \\
&= -\frac{(2-\lambda_z)}{3} R_2 - \frac{(1+\lambda_z)}{3} R_3.
\end{aligned} \tag{51}$$

The limiting rates are R_2 and R_3, which therefore constrains λ_z to the range

$$-1 \le \lambda_z \le 2. \tag{52}$$

The damping has equal contributions from R_2 and R_3 for $\lambda_z = 1/2$, with a larger contribution from either R_2 or R_3 if λ_z is less than or greater than 1/2, respectively.

The dependence of z_1 on $\boldsymbol{\omega}_e$ and R_δ, calculated according to Eqs. (C6), is shown in Fig. 2, where contours of λ_z are plotted as a function of λ_{12} and λ_3. As discussed earlier, there is only one real root for $\lambda_3 > 1$. When $\lambda_3 \le 1$, there is also a single real root for values of λ_{12} outside the narrow bounds that define critical damping. Within these bounds where the solutions represent overdamping, any of the three real roots can be designated as z_1, with $z_\pm$ from Eq. (C6c) giving the other two. For $\omega_{12} = 0$, the relaxation rate is R_3 (i.e., $\lambda_z = 2$), independent of the offset parameter λ_3, as is well-known. As ω_{12} increases for fixed ω_3, the relaxation rate approaches R_2 ($\lambda_z = -1$), with the drop-off from $\lambda_z = 2$ becoming increasingly steep at lower values of ω_3. For the other roots in which $\mathrm{Re}(z_\pm) = -1/2\, z_1$, the upper limit in Eq. (52) becomes 1/2.

2. A linear relation for the roots

Equation (19) evaluated at the real root z_1 yields the linear relation

$$\tilde{c}_0 = -z_1 \tilde{c}_1 - z_1^3. \tag{53}$$

The slope and intercept are determined by z_1. Substituting the expressions for $\tilde{c}_0$ and $\tilde{c}_1$ given in Eq. (49), rearranging, and collecting terms after writing $9\lambda_z = 6\lambda_z + 3\lambda_z$ gives

$$\lambda_{12} = m_s\, \lambda_3 + \lambda_{12}^{\mathrm{int}} \tag{54}$$

with slope m_s and intercept $\lambda_{12}^{\mathrm{int}}$ given by

$$m_\mathrm{s} = \frac{2-\lambda_z}{1+\lambda_z}, \qquad y_{12}^{\mathrm{int}} = 3(2-\lambda_z)(1+\lambda_z). \tag{55}$$

There is thus a simple graphical representation for the value of the root z_1 as a function of the physical parameters $\omega_{12}, \omega_3, R_\delta$. There are a continuum of field values for a given R_δ that give the same z_1. Lines of constant z_1 as a function of λ_{12} and λ_3 become hyperbolas when Eq. (54) is rewritten in terms of $\omega_{12}^2, \omega_3^2, R_\delta^2$ using Eq. (47). A similar graphical analysis for any cubic polynomial with real coefficients reveals the parameter space yielding either one real and two complex conjugate roots, three real roots, or degenerate roots.

V. INTUITIVE REPRESENTATIONS OF SYSTEM DYNAMICS

There are few, if any, simple models that interpret the solutions. In this section, we develop four, three of which are completely general. The reader is also referred to an abstract model for the on-resonance ($\omega_3 = 0$) geometrical structure of OBE dynamics [36].

In most cases, the parameters of the Bloch equation yield three distinct roots for the characteristic polynomial $p(s)$ of Eq. (17), described as cases (i) and (ii) in Sec. III A. Exceptions were considered in more detail in Sec. IV for the OBE. To provide additional physical insight, we develop a straightforward vector model for the trajectory of $M(t)$ given by Eq. (10). The model is the 3D analogue to the dynamics of a single damped harmonic oscillator. As noted in section II A, a parametric plot of $\dot{x}(t)$ as a function of $x(t)$ is a decaying spiral in the phase plane (for underdamped motion). To make this connection more explicit, we first develop a damped oscillator model for the Bloch equation. Modeling dissipative processes in this manner provides a new perspective within the context of well-understood coupled harmonic oscillations. Fresh perspectives can yield new insights. Conversely, the dynamics of a damped oscillator can be represented by a Bloch-like equation for a single rotor in two dimensions. The comparison provides insight towards developing an easily visualized vector model of Bloch equation dynamics. An alternative vector model is then also considered.

A. The Bloch equation as a system of coupled oscillators

Any quantum N-level system can be represented as a system of coupled harmonic oscillators [26], albeit requiring negative or even antisymmetric couplings. The Bloch equation is perhaps particularly interesting, since it incorporates dissipation for the most elementary case, i.e., 2-level systems.

To compare the Bloch equation to Eq. (5) for the damped harmonic oscillator, first eliminate the inhomogeneous term from either equation by the appropriate shift of coordinates, as discussed previously. Differentiating Eq. (9) with respect to time, writing Γ as the sum of diagonal matrix $(\Gamma_\mathrm{d})_{ii} = R_i$ and off-diagonal elements Γ_od, and substituting $\dot{\mathcal{M}} = -\Gamma\mathcal{M}$ in the resulting Γ_od term gives, for $\Lambda^2 \equiv -\Gamma_\mathrm{od}\Gamma$,

$$\ddot{\mathcal{M}}(t) + \Gamma_\mathrm{d}\dot{\mathcal{M}} + \Lambda^2\mathcal{M} = 0 \tag{56}$$

with

$$\Lambda^2 = -\begin{bmatrix} \Gamma_{12}\Gamma_{21} + \Gamma_{13}\Gamma_{31} & \Gamma_{13}\Gamma_{32} + \Gamma_{12}R_2 & \Gamma_{12}\Gamma_{23} + \Gamma_{13}R_3 \\ \Gamma_{31}\Gamma_{23} + \Gamma_{21}R_1 & \Gamma_{12}\Gamma_{21} + \Gamma_{23}\Gamma_{32} & \Gamma_{13}\Gamma_{21} + \Gamma_{23}R_3 \\ \Gamma_{21}\Gamma_{32} + \Gamma_{31}R_1 & \Gamma_{31}\Gamma_{12} + \Gamma_{32}R_2 & \Gamma_{13}\Gamma_{31} + \Gamma_{23}\Gamma_{32} \end{bmatrix}$$

$$\xrightarrow{\mathrm{OBE}} -\begin{bmatrix} -(\omega_2^2+\omega_3^2) & \omega_1\omega_2 + \omega_3 R_2 & \omega_1\omega_3 - \omega_2 R_3 \\ \omega_1\omega_2 - \omega_3 R_1 & -(\omega_1^2+\omega_3^2) & \omega_2\omega_3 + \omega_1 R_3 \\ \omega_1\omega_3 + \omega_2 R_1 & \omega_2\omega_3 - \omega_1 R_2 & -(\omega_1^2+\omega_2^2) \end{bmatrix}. \tag{57}$$

Referring to the system of three coupled oscillators in Fig. 4, the displacement r_i of mass m_i from equilibrium is equal to $\mathcal{M}_i$. The natural frequency of m_i is $(\Lambda^2)_{ii}$, with associated damping coefficient R_i multiplying component $\mathcal{M}_i$. For unit masses, the force equation for m_i gives $(\Lambda^2)_{ii} = k_{ii} + \sum_{j\neq i} k_{ij}$ and a simple solution for the k_{ii}. Up to this point, a mechanical implementation of the oscillator system would be possible. However, the coupling constants $k_{ij} = -(\Lambda^2)_{ij}$ are asymmetric, which is a distinguishing feature of two-level systems with dissipation and can not be implemented with a system of springs or other mechanical contrivances.

The effect of asymmetric couplings seen more clearly by keeping Γ intact thoughout the previous derivation, giving

$$\ddot{\mathcal{M}}(t) - \Gamma^2\mathcal{M} = 0. \tag{58}$$

The elements of Γ^2 are similar to those of Λ^2. They differ by the addition of R_i^2 to each diagonal element of

$-\Lambda^2$ and $R_i\Gamma_{ij}$ to each element of $-(\Lambda)_{ij}$. This version of the oscillator model is in the form of ideal, frictionless couplings but is, nonetheless, damped. How might dissipation arise in a "frictionless" system?

The couplings k_{ij} are still asymmetric. For a given positive k_{ij}, a positive displacement of mass m_j results in a positive force on m_i. The resulting positive displacement of m_i provides a different force on m_j due to $k_{ji} \neq k_{ij}$. Energy transferred from m_j to m_i is not reciprocally transferred back from m_i to m_j, and the motion is quenched. Asymmetric couplings can act as a negative feedback mechanism to curb system oscillations in the models represented in Eq. (56) and Eq. (58), similar to pushing a swing at a nonresonant frequency. Damped solutions are obtained in both models even if $R_i \to 0$ in the diagonal elements of $(\Lambda)^2$ or Γ^2.

Further insight is obtained by converting the simple damped oscillator to a system of coupled first-order differential equations, i.e., in the same format as the Bloch equation. Defining a two-element vector $\boldsymbol{r}$ with components $r_1 = x - g/\omega_0^2$ and $r_2 = \dot{x}$ gives

$$\begin{aligned}\dot{\boldsymbol{r}}(t) &= -\begin{pmatrix} 0 & -1 \\ \omega_0^2 & 2b \end{pmatrix}\boldsymbol{r}(t) \\ &= -\tilde{\Lambda}\,\boldsymbol{r}(t) \end{aligned} \tag{59}$$

and solution $\boldsymbol{r}(t) = e^{-\tilde{\Lambda}t}\boldsymbol{r}(0)$. The propagator is easily calculated directly or deduced using the solution in Eq. (6). Either way, the action of the propagator on any initial state $\boldsymbol{r}(0)$ is a decaying spiral in the (r_1, r_2)-plane, as discussed previously. One might then wonder whether there is a similarly simple vector model of system dynamics for the Bloch equation.

B. Bloch equation dynamics: simple limiting cases

As a point of departure, consider first the OBE. For simple limiting cases, the dynamics are already well known and readily visualized. In the absence of relaxation, i.e., all $R_i = 0$, any magnetization vector $\mathcal{M}$ rotates about the total effective field $\boldsymbol{\omega}_e$ at constant angular frequency ω_e. The time evolution of a vector under the action of the propagator has a simple solution in a coordinate system rotated to align one of the axes with the effective field. The component of $\mathcal{M}$ along $\boldsymbol{\omega}_e$ is constant, and the components in the plane perpendicular to $\boldsymbol{\omega}_e$ rotate at angular frequency ω_e in the plane. By contrast, the solution for each component $\mathcal{M}_i(t)$ in the standard (x_1, x_2, x_3)-coordinate system is more complicated, and it is not immediately apparent by inspection that the solution is a rotation.

If the relaxation is switched on with equal rates $R_i = R$, the diagonal relaxation matrix $R\mathbb{1}$ commutes with the remaining rotation matrix. The simplification it affords has not been acknowledged in any of the previously cited solutions. The solution is a simple dynamic scaling e^{-Rt} of the rotating vector $\mathcal{M}$, as obtained by Jaynes [31] via a more circuitous route. In addition, for $\omega_{12} = 0$ and $R_1 = R_2 \neq R_3$, the relaxation matrix still commutes with the rotation about nonzero ω_3. The evolution is then in terms of noninteracting longitudinal and transverse components. We have exponential decay $e^{-R_3 t}$ of component $\mathcal{M}_3$ and decay $e^{-R_2 t}$ of the transverse component $\mathcal{M}_{12}$, which rotates at angular frequency ω_3 in the plane perpendicular to ω_3, as illustrated in Fig. 3a. In the case of pure relaxation, with all the field components $\omega_i = 0$, the solution is a non-oscillatory exponential decay $e^{-R_i t}$ for each component $\mathcal{M}_i$ along coordinate axis x_i.

C. Bloch equation dynamics: a more general vector model

With the exception of the above simple cases, there has been no analogous picture of system dynamics when the rotation and relaxation do not commute. The combined, noncommutative action of arbitrary fields and dissipation rates appears to require something more complex. Yet, the simple visual model shown in Fig. 3a, which is comprised of independent relaxation and rotation elements, is readily extended to the general case of arbitrary Γ when viewed in an appropriate coordinate system. This requires the action of the propagator $e^{-\Gamma\, t}$ on an arbitrary vector.

The eigensystem for Γ is considered in sections that follow, but one can substitute notation for the partitioned matrix Γ_p in the expressions which are derived, since, as defined in Eq. (32), the matrices differ by a constant $\bar{R}$ times the identity matrix. The difference in the eigenvalues is also $\bar{R}$, from Eqs. (24) and (25). Thus $-\Gamma$ and $-\Gamma_\mathrm{p}$ have the same eigenvectors $\boldsymbol{s}_i \equiv \boldsymbol{z}_i$. Simple analytical expressions for the eigenvectors and other constituents of the model are derived in Appendix F. Each (unnormalized) eigenvector, which can assume different analytical forms depending on the scaling, comprises the columns of $\operatorname{adj} A(s_i) = \operatorname{adj} A_\mathrm{p}(z_i)$, as derived in Appendix B. This provides a useful method for calculating an eigenvector, especially in symbolic form as a function of matrix parameters.

1. One real, two complex conjugate roots

The solution for each component $\mathcal{M}_i$ is known to be a combination of oscillation and bi-exponential decay [6], as is also evident from the propagator derived in Eq. (15). The underlying simplicity of the system dynamics can be demonstrated starting with the eigensystem for Γ (or, alternatively, Γ_p, as noted above).

The real eigenvalue s_1 of $-\Gamma$ has a real eigenvector $\boldsymbol{s}_1$ which can be used as one axis of a physical coordinate system, but the complex roots s_+ and $s_- = s_+^*$ have associated complex eigenvectors $\boldsymbol{s}_+$ and $\boldsymbol{s}_- = \boldsymbol{s}_+^*$.

Define the real vectors

$$\begin{aligned} \tilde{\boldsymbol{s}}_1 = \boldsymbol{s}_1, \qquad \tilde{\boldsymbol{s}}_2 &= \tfrac{1}{2}\left(\boldsymbol{s}_+ + \boldsymbol{s}_-\right), \qquad & \tilde{\boldsymbol{s}}_3 &= -\frac{i}{2}\left(\boldsymbol{s}_+ - \boldsymbol{s}_-\right) \\ &= \mathrm{Re}\left[\boldsymbol{s}_+\right], & &= \mathrm{Im}\left[\boldsymbol{s}_+\right]. \end{aligned} \tag{60}$$

The eigenvectors above are most generally not orthogonal for arbitrary Γ, but they are linearly independent, given the distinct eigenvalues. The set $\{\tilde{\boldsymbol{s}}_1, \tilde{\boldsymbol{s}}_2, \tilde{\boldsymbol{s}}_3\}$ is then also linearly independent and can be used as an alternative physical basis for describing the system evolution. The new coordinate system will most generally also be non-orthogonal (oblique). System states and operators are transformed between bases in the usual fashion by a matrix P comprised of the $\{\tilde{\boldsymbol{s}}_i\}$ entered as column vectors. Vector $\tilde{\mathcal{M}}$ and the propagator in the new basis are given by

$$\begin{aligned} \tilde{\mathcal{M}} &= P^{-1}\mathcal{M} \\ e^{-\tilde{\Gamma}t} &= P^{-1}e^{-\Gamma t}P \\ &= e^{-(P^{-1}\Gamma P)t}, \end{aligned} \tag{61}$$

with P invertible since the $\tilde{\boldsymbol{s}}_i$ are linearly independent.

The potentially tedious process of calculating $e^{-\tilde{\Gamma}\,t}$ from Eq. (61) can be bypassed, with $e^{-\tilde{\Gamma}\,t}$ deduced from the action of Γ on its eigenvectors (see Appendix F). In terms of constants

$$\tilde{s}_1 = -(\bar{R} - z_1), \qquad \tilde{s}_{23} = -(\bar{R} + z_1/2), \tag{62}$$

and ϖ of Eq. (22), the solution $\tilde{\mathcal{M}}(t) = e^{-\tilde{\Gamma}t}\tilde{\mathcal{M}}(0)$ for the time dependence of state vector $\tilde{\mathcal{M}}$ in the new basis is found to be

$$\begin{aligned} \tilde{\mathcal{M}}(t) = &\begin{pmatrix} e^{\tilde{s}_1 t} & 0 & 0 \\ 0 & e^{\tilde{s}_{23} t} & 0 \\ 0 & 0 & e^{\tilde{s}_{23} t} \end{pmatrix} \times \\ &\begin{pmatrix} 1 & 0 & 0 \\ 0 & \cos\varpi t & \sin\varpi t \\ 0 & -\sin\varpi t & \cos\varpi t \end{pmatrix} \tilde{\mathcal{M}}(0) \end{aligned} \tag{63}$$

Viewed in the $\{\tilde{\boldsymbol{s}}_i\}$ coordinate system, $\mathcal{M}$ evolves according to independent, commuting rotation and relaxation operators. The component of $\mathcal{M}$ along $\tilde{\boldsymbol{s}}_1$ (i.e., $\tilde{\mathcal{M}}_1$) decays at the rate $\tilde{s}_1 = \bar{R} - z_1$, while components in the $(\tilde{\boldsymbol{s}}_2, \tilde{\boldsymbol{s}}_3)$-plane rotate in the plane and decay at the rate $\tilde{s}_{23} = \bar{R} + z_1/2$. Thus, even in the most general case of three unequal rates R_1, R_2, R_3, there emerges a single "planar" relaxation rate R_{2s} and a new "longitudinal" relaxation rate R_{1s} defined as

$$R_{1s} = |\tilde{s}_1| = 1/T_{1s} \quad \text{and} \quad R_{2s} = |\tilde{s}_{23}| = 1/T_{2s}. \tag{64}$$

Defining $\tilde{\mathcal{M}}(t)$ as the state $\boldsymbol{M}(t) - \boldsymbol{M}_\infty$ expressed in the $\{\tilde{\boldsymbol{s}}_i\}$ coordinates and working backwards from Eq. (63) gives the Bloch equation in this basis as

$$\begin{aligned} &\frac{d}{dt}\,\tilde{\mathcal{M}}(t) + \tilde{\Gamma}\,\tilde{\mathcal{M}}(t) = 0 \\ &\tilde{\Gamma} = \begin{pmatrix} R_{1s} & 0 & 0 \\ 0 & R_{2s} & \varpi \\ 0 & -\varpi & R_{2s} \end{pmatrix} \end{aligned} \tag{65}$$

The diagonal matrix consisting of the relaxation rates R_{is} commutes with the matrix of off-diagonal elements. This anti-symmetric matrix comprised of $\pm\varpi$ generates a rotation about $\tilde{\boldsymbol{s}}_1$, and one immediately obtains the solution given in Eq. (63). This extends the result of Sec. V B for the simple OBE with $\omega_{12} = 0$ and $R_1 = R_2 \neq R_3$ to completely general Bloch equations.

We should emphasize that one has considerable latitude in the choice of $\tilde{\boldsymbol{s}}_2$ and $\tilde{\boldsymbol{s}}_3$, since all components in the plane they define decay at the same rate. Rotating these coordinate axes in the plane by any angle results in an equally valid set of axes for representing the dynamics. The vectors $\tilde{\boldsymbol{s}}_2$ and $\tilde{\boldsymbol{s}}_3$ constructed from a particular column in the coefficient matrices of Eq. (F7) are related to axes constructed from one of the other columns by a rotation (excepting when one of the columns returns the irrelevant zero vector). By contrast, $\tilde{\boldsymbol{s}}_1$ defines the unique axis for longitudinal decay, so the $\tilde{\boldsymbol{s}}_1$ chosen from different columns must be related by a scale factor.

Note also that the rotation in the plane is *not* at a constant angular frequency ϖ unless $\tilde{\boldsymbol{s}}_2$ and $\tilde{\boldsymbol{s}}_3$ are orthogonal. A component aligned with $\tilde{\boldsymbol{s}}_2$ rotates to $\tilde{\boldsymbol{s}}_3$ during a time defined by the condition $\varpi t = \pi/2$, then rotates from there to $-\tilde{\boldsymbol{s}}_2$ in the same time. In an oblique coordinate system, the rotations are through different angles in the same time, so clearly the angular frequency of the rotation in physical space is not constant.

Although Eq. (63) is perhaps reminiscent of a normal mode analysis, recall that the normal mode coordinates are the eigenvectors of $-\Gamma$, two of which are complex and, hence, unphysical. The physical $\{\tilde{\boldsymbol{s}}_i\}$ coordinate system is comprised of linear combinations of the eigenvectors, which have distinct eigenvalues. The $\{\tilde{\boldsymbol{s}}_i\}$ as a set are therefore not the eigenvectors of $-\Gamma$ (although $\{\tilde{\boldsymbol{s}}_1\}$ is, by definition).

2. Three real roots

In this case, all the eigenvectors are real and the new basis is simply the eigenbasis $\{\boldsymbol{s}_1, \boldsymbol{s}_2, \boldsymbol{s}_3\}$ obtained from the roots

$$s_i = -(\bar{R} - z_i) \tag{66}$$

defined in Eq. (24). The real roots z_i are obtained for $\varpi^2 < 0$ in Eq. (22). Substituting $\varpi \to i\mu$ in Eq. (21) gives $z_{2,3} = -1/2\, z_1 \mp \mu$.

The matrix Γ is obviously diagonal in its eigenbasis, and, by extension, so is the propagator in this basis. Thus

$$\tilde{\mathcal{M}}(t) = \begin{pmatrix} e^{s_1 t} & 0 & 0 \\ 0 & e^{s_2 t} & 0 \\ 0 & 0 & e^{s_3 t} \end{pmatrix} \tilde{\mathcal{M}}(0) \qquad (67)$$

Each component of $\mathcal{M}$ along $\tilde{\boldsymbol{s}}_i$ decays at the rate determined by s_i. In contradistinction to the rates that emerge from the oscillatory solutions, here, even in the typical case of equal transverse rates $R_1 = R_2$ and longitudinal rate R_3, we find three distinct rates

$$R_{is} = |s_i| = 1/T_{is} \qquad (68)$$

due to the coupling of the field with the relaxation processes.

Given $e^{-\tilde{\Gamma} t}$ as obtained in Eq. (63) or (67), the propagator in the standard coordinate basis is $e^{-\Gamma t} = P e^{-\tilde{\Gamma} t} P^{-1}$ from Eq. (61). One obtains a simple, factored solution for the propagator derived by different methods in Sec. III. The physical interpretation of the dynamics is correspondingly simple, with oscillation frequencies and decay rates hinging upon the primary real root z_1. The dependence of this root on the fields and relaxation rates has been shown previously in Fig. 2.

3. *Degenerate roots*

The vector model approach to obtaining the propagator is only applicable to the case of distinct eigenvalues. Degenerate eigenvalues do not give the linearly independent eigenvectors necessary to define a new coordinate system. However, the degeneracies are a relatively trivial component of the parameter space, at least for the OBE, as shown in Fig. 1. Moreover, the solution has to be continuous as the degeneracies are approached, with a smooth transition from oscillatory, decaying solutions to pure decay as one crosses the parameter-space boundary identifying the degenerate solutions.

4. *Discussion and representative examples*

The solutions of Sec. III are represented in the standard coordinate system, expressed in general form for arbitrary driving matrix Γ. Here, they are applied to specific physical examples applicable to the OBE, with $R_1 = R_2$. The trajectories of initial states under the action of the propagator are plotted to illustrate the underlying simplicity of the dynamics and corroborate the alternative coordinate system that defines the vector model. Parameters for the examples are chosen to demonstrate the damping and rotation that are characteristic of the dynamics for all but a small region of the parameter space. A purely damped solution and model dynamics given by Eq. (67) is rather featureless, by comparison. Unless stated otherwise, the first column of adj $A_{\rm p}$ is chosen to calculate the eigenvectors and coordinate basis $\{\tilde{\boldsymbol{s}}_i\}$.

a. Free precession, $\boldsymbol{\omega}_e = (0, 0, \omega_3)$ When the only field in the rotating frame is the offset from resonance, ω_3, the matrix $\Gamma_{\rm p}$ is the sum of a diagonal relaxation matrix and the matrix which generates a rotation about ω_3. Since they commute, the propagator factors into the product of exponential decay and a rotation, leading to the standard interpretation of the dynamics discussed previously in Sec. V B. This example also provides a simple illustration of the more general vector model. The eigenvalues are easily obtained as $z_1 = 2R_\delta$ and $z_\pm = -R_\delta \pm i\omega_3$. Then Eq. (F6) gives, upon identifying $\varpi \equiv \omega_3$ and eliminating common factors in individual columns,

$$\tilde{\boldsymbol{s}}_1 \leftarrow \begin{pmatrix} 0 & 0 & 0 \\ 0 & 0 & 0 \\ 0 & 0 & 1 \end{pmatrix} \qquad \tilde{\boldsymbol{s}}_2 \leftarrow \begin{pmatrix} \omega_3 & -3R_\delta & 0 \\ 3R_\delta & \omega_3 & 0 \\ 0 & 0 & 0 \end{pmatrix}$$
$$\tilde{\boldsymbol{s}}_3 \leftarrow \begin{pmatrix} 3R_\delta & \omega_3 & 0 \\ -\omega_3 & 3R_\delta & 0 \\ 0 & 0 & 0 \end{pmatrix}. \qquad (69)$$

As noted earlier, there is always only one unique nonzero result for $\tilde{\boldsymbol{s}}_1$, with any apparent differences between columns simply a matter of scale. The nonzero columns for $\tilde{\boldsymbol{s}}_2$ are orthogonal, as are those of $\tilde{\boldsymbol{s}}_3$. The columns thus differ, as expected, by a rotation in the $(\tilde{\boldsymbol{s}}_2, \tilde{\boldsymbol{s}}_3)$-plane, in this case by 90°. Choosing the second column and a left-handed rotation by $\phi = \tan^{-1}(3R_\delta/\omega_3)$ or the first column and a right-handed rotation by $90 - \phi$ gives the more typical result $\tilde{\boldsymbol{s}}_2 = (0, 1, 0)$ and $\tilde{\boldsymbol{s}}_3 = (1, 0, 0)$ depicted in Fig. 3a. The model dynamics for an initial state $\mathcal{M}_0$ is a spiral about $\boldsymbol{\omega}_e$, which is aligned along the z-axis, with rotation at constant angular frequency ω_e in the (x, y)-plane, as required. The relaxation rate obtained from Eq. (51) or Eq. (62) for $z_1 = 2R_\delta$, with $\lambda_z = 2$, is $R_{1s} = R_3$, while the roots $z_\pm$ with $\lambda_z = -1$ give $R_{2s} = R_2$, as expected.

b. On resonance, $\boldsymbol{\omega}_e = (\omega_1, \omega_2, 0)$ The effective field is now in the transverse plane instead of along the z-axis as in the preceding example. Yet there has been no visual intuition of the dynamics for this simple change in the orientation of $\boldsymbol{\omega}_e$. This is the simplest example for the new vector model. What does it predict?

The root $z_1 = -R_\delta$, and $\varpi^2 = \omega_e^2 - (3/2R_\delta)^2$ from Eq. (G14). The associated eigenvector $\tilde{\boldsymbol{s}}_1$ is obtained by inspection from Eq. (F5), with $\tilde{\boldsymbol{s}}_2$ and $\tilde{\boldsymbol{s}}_3$ obtained from Eqs. (F6) and (F7), giving

$$\tilde{\boldsymbol{s}}_1 = \begin{pmatrix} \omega_1 \\ \omega_2 \\ 0 \end{pmatrix} \qquad \tilde{\boldsymbol{s}}_2 = \begin{pmatrix} -\omega_2 \\ \omega_1 \\ -\frac{3}{2}R_\delta \end{pmatrix} \qquad \tilde{\boldsymbol{s}}_3 = \begin{pmatrix} 0 \\ 0 \\ 1 \end{pmatrix}. \qquad (70)$$

Thus, on resonance, the propagator still generates a spiral about the effective field $\boldsymbol{\omega}_e = \tilde{\boldsymbol{s}}_1$ with precession in the $(\tilde{\boldsymbol{s}}_2, \tilde{\boldsymbol{s}}_3)$-plane orthogonal to $\tilde{\boldsymbol{s}}_1$. However, as considered in section V C 1, the rotation frequency driven by ϖ is not constant, since $\tilde{\boldsymbol{s}}_2$ is not perpendicular to $\tilde{\boldsymbol{s}}_3$. The deviation from orthogonality, determined by the third component of $\tilde{\boldsymbol{s}}_2$, is small for fields that are large compared to R_δ. The respective decay rates R_{1s} and R_{2s} are R_2 and $1/2(R_2+R_3)$, using $\lambda_z=-1$ and $\lambda_z=1/2$ as determined from z_1 and $-z_1/2$. Components along $\tilde{\boldsymbol{s}}_1$, i.e., in the (x,y)-plane, decay at the usual spin-spin relaxation rate, as would be expected. Components rotating in the plane orthogonal to $\tilde{\boldsymbol{s}}_1$ experience equal influence, on average, from their projection onto the longitudinal z-axis defining ω_3 and their projection into the (x,y)-plane, so one might predict from the model that they decay at the average of the usual spin-spin and longitudinal relaxation rates. These values for the decay rates have been obtained previously as elements of the solution in the standard coordinate system [6] without the physical interpretation presented here.

The trajectory for an initial state $\mathcal{M}_0$ due to the action of propagator $e^{-\Gamma t}$ with $\boldsymbol{\omega}_e=(\omega_1,0,0)$ and nonzero relaxation is shown in Fig. 3b. Values of the parameters are given in the caption. For nonzero ω_2, the figure is simply rotated about the z-axis by angle $\phi=\tan^{-1}(\omega_2/\omega_1)$. The state $\mathcal{M}_0$ has been chosen with equal components parallel and orthogonal to $\boldsymbol{\omega}_e$ to most clearly illustrate the dynamics predicted by the vector model. The slight misalignment between $\tilde{\boldsymbol{s}}_2$ and the y-axis, which makes $\tilde{\boldsymbol{s}}_2$ and $\tilde{\boldsymbol{s}}_3$ nonorthogonal, is evident in the figure and becomes more prominent as the magnitude of the field, ω_{12}, is reduced relative to R_δ.

c. Off resonance, general $\boldsymbol{\omega}_e$ Most generally, $\tilde{\boldsymbol{s}}_1$ is not aligned with $\boldsymbol{\omega}_e$. Dividing column j of the matrix in Eq. (F5) by (nonzero) ω_j quantifies the degree to which $\tilde{\boldsymbol{s}}_1$ deviates from $\boldsymbol{\omega}_e$ due to the coupling between the fields and the relaxation rates R_i. The result is an expression of the form $\boldsymbol{s}_1=\boldsymbol{\omega}_e+\delta\boldsymbol{v}$, where vector $\delta\boldsymbol{v}$ is comprised of the second term in each row of the j^{th} column divided by ω_j.

In addition, $\tilde{\boldsymbol{s}}_1$ is typically not orthogonal to the $(\tilde{\boldsymbol{s}}_2,\tilde{\boldsymbol{s}}_3)$-plane. One then has to further modify intuitions developed from orthogonal coordinate systems. For example, in Fig. 3c, $\mathcal{M}_0$ is aligned with the normal to the $(\tilde{\boldsymbol{s}}_2,\tilde{\boldsymbol{s}}_3)$-plane. It therefore has no orthogonal projection in the plane and might naively be expected to have no evolution in the plane. However, $\tilde{\boldsymbol{s}}_1$ is distinctly different than the normal, and $\mathcal{M}_0$ is the vector sum of a component along $\tilde{\boldsymbol{s}}_1$ and a component parallel to the plane, which are the quantities relevant for the vector model. As shown in the figure, the parallel component rotates and decays in the plane while the component along $\tilde{\boldsymbol{s}}_1$ strictly decays. Similarly, $\mathcal{M}_0$ orthogonal to $\tilde{\boldsymbol{s}}_1$ as in Fig. 3d nonetheless has a component along $\tilde{\boldsymbol{s}}_1$ in the oblique coordinates. This component decays to generate the spiral shown in the figure.

Contrast this with the dynamics viewed in standard coordinates, where the solution for each component $\mathcal{M}_i(t)$ is an oscillation combined with relaxation at two separate rates. As in simpler examples, it can be decoupled into two independent dynamical systems, one of which rotates in a plane and decays at one rate and another which decays along a fixed axis, albeit in an oblique coordinate system.

The deviation of $\tilde{\boldsymbol{s}}_1$ from the normal to the plane is quantified in Appendix F for $\boldsymbol{\omega}_{12}$ of either x- or y-phase and for $\omega_1=\omega_2=\omega_3$.

D. Alternative vector model

The Bloch equation, considered here in matrix form, is typically represented in vector form. Its physics is the torque on a magnetic moment in a magnetic field subject to relaxation of the magnetization. The effects of this physics on the OBE solution can be made more explicit by returning to the original vector operations, motivated by the treatment in Jaynes [31] for the rotation of a vector about the field.

Partition $\Gamma_{\rm p}$ into its diagonal elements $R_{i\rm p}$ and off-diagonal ω_i, writing $\Gamma_{\rm p}=\mathcal{R}_{\rm p}+\Omega$. The diagonal matrix $\mathcal{R}_{\rm p}$ scales each component $\mathcal{M}_i$ of a vector $\mathcal{M}$ by $R_{i\rm p}$, and Ω implements the cross product $(-\boldsymbol{\omega}_e\times\ )$. According to Eq. (30), the propagator acting on $\mathcal{M}$ generates three separate vectors $\boldsymbol{v}_n=\Gamma_{\rm p}^n\mathcal{M},(n=0,1,2)$, which can be represented starting with $\boldsymbol{v}_0=\mathcal{M}$ as

$$\begin{aligned}\Gamma_{\rm p}\,\mathcal{M}&=(\mathcal{R}_{\rm p}+\Omega)\,\boldsymbol{v}_0\\&=(\mathcal{R}_{\rm p}\,\mathcal{M})-\,(\boldsymbol{\omega}_e\times\mathcal{M})\\&=\boldsymbol{v}_1\end{aligned}$$

$$\begin{aligned}\Gamma_{\rm p}^2\,\mathcal{M}&=(\mathcal{R}_{\rm p}\,+\Omega)\,\boldsymbol{v}_1\\&=(\mathcal{R}_{\rm p}^2\,\mathcal{M})-\,\mathcal{R}_{\rm p}\,(\,\boldsymbol{\omega}_e\times\mathcal{M})-\,\boldsymbol{\omega}_e\times(\mathcal{R}_{\rm p}\mathcal{M})\,+\\&\quad\ \boldsymbol{\omega}_e\times(\boldsymbol{\omega}_e\times\mathcal{M})\\&=(\mathcal{R}_{\rm p}^2\,\mathcal{M})-\mathcal{R}_{\rm p}\,(\,\boldsymbol{\omega}_e\times\mathcal{M})-\,\boldsymbol{\omega}_e\times(\mathcal{R}_{\rm p}\mathcal{M})\,+\\&\quad\ \boldsymbol{\omega}_e\,(\boldsymbol{\omega}_e\cdot\mathcal{M})-\omega_e^2\,\mathcal{M}\\&=\boldsymbol{v}_2\end{aligned}\qquad(71)$$

Each succeeding $\boldsymbol{v}_n$ is a nonuniform scaling of the previous $\boldsymbol{v}_{n-1}$ added to a vector $(\boldsymbol{v}_{n-1}\times\boldsymbol{\omega}_e)$ that is orthogonal to $\boldsymbol{v}_{n-1}$. The time dependence of $\boldsymbol{v}_n$ is given by the associated term $a_n(t)e^{-\bar{R}t}$ found in Eqs. (37–39). The $a_n(t)$ are factored as the product of a matrix $W(z_1)$ and vector $\boldsymbol{u}(t)$. Each $a_n(t)$ is merely a different linear combination of the same three simple functions $u_i(t)$ that comprise the components of $\boldsymbol{u}$, weighted according to the corresponding elements from row n of the matrix W. A given $\boldsymbol{v}_n(t)$ thus maintains a fixed orientation, changing length with a time dependence consisting of the different weightings of the $u_i(t)$ for different $\boldsymbol{v}_n$. The trajectory $\mathcal{M}(t)=\sum_n\boldsymbol{v}_n(t)$ can thus be represented in terms of the decaying oscillations of three vectors fixed in place.

Alternatively, expand $(\mathbb{1},\Gamma_p,\Gamma_p^2)\,W(z_1)\boldsymbol{u}(t)$ and group terms of the same time dependence $u_i(t)$. The propagator applied to $\mathcal{M}$ gives three different linear combinations of the $\boldsymbol{v}_n$, with a time dependence $u_i(t)$ for the i^{th} combination. The resulting interpretation of $\mathcal{M}(t)$ is similar to the previous paragraph, but the functional form of the decaying oscillations is simpler using this different set of vectors.

VI. CONCLUSION

A more comprehensive solution of the Bloch equation has been presented together with intuitive visual models of its dynamics. The solution is valid for arbitrary system parameters, yet is simpler than previous solutions. It can be expressed as the product of three separate terms: one which depends directly on the physical parameters of the problem through the driving matrix Γ, a term that depends on its eigenvalues, and a term that gives the time dependence, which in turn is solely a function of the eigenvalues. Moreover, the time evolution of the system as a function of the physical parameters has been made more explicit and apparent.

System dynamics depend critically on the eigenvalues, with (i) oscillatory, underdamped evolution for one real and two complex-conjugate values, (ii) non-oscillatory, overdamped evolution for three real values, and (iii) non-oscillatory, critically damped evolution for doubly or triply degenerate (real) values. The damping rates and the frequency driving the oscillatory behavior have been reduced to simple functions of a primary, real eigenvalue that is obtained as a straightforward function of the system parameters. For the conventional Bloch equation, simple quantitative relations have been derived that delineate the three categories of dynamical behavior in terms of the physical parameters. A linear relation has also been derived in this case relating critical system parameters to the primary eigenvalue, which provides a straightforward graphical realization of the damping rates and frequency for a given physical configuration.

An intuitive dynamical model developed here transforms the general Bloch equation to a frame in which damping commutes with a rotation, providing a propagator for the time evolution of the system that is the product of a rotation times a decay, in either order. The decay rates in this frame result from interaction/coupling of the fields with the spin-lattice and spin-spin relaxation processes. The model was motivated by well-known visual models for simple conventional cases such as equal relaxation rates or free precession (no fields transverse to the longitudinal, z-axis). The system state in such cases rotates about the effective field, with concurrent exponential decay of the longitudinal and transverse components. The extended model retains the same essential features: rotation, exponential decay of the invariant component in the rotation (analogous to the longitudinal axis), and a separate decay of the rotating components in an analogous transverse plane. The model also includes solely damped solutions (i.e., no rotation). An alternative vector model has also been provided, as well as a representation of the Bloch equation as a system of coupled, damped harmonic oscillators. The net result of the solutions and models is a framework for more direct physical insight into the dynamics of the Bloch equation.

ACKNOWLEDGMENTS

The author gratefully acknowledges support from the National Science Foundation under Grant CHE-1214006.

Appendix A: Proof of Eq. (27)

Consider a general 3×3 matrix Υ with characteristic polynomial $p(s) = \det(s\mathbb{1} - \Upsilon) = \sum_{j=0}^{3} c_j s^j$ and polynomials $p_j(s)$ derived from it as defined in Eq. (31). The claim is that

$$\mathrm{adj}\,(s\,\mathbb{1} - \Upsilon) = \sum_{j=0}^{2} p_j(s)\Upsilon^j. \qquad \text{(A1)}$$

Note first that $\sum_{j=0}^{2} p_j(s)\Upsilon^j = \sum_{j=0}^{2} p_j(\Upsilon)s^j$, as is easily verified by expanding the terms. Then Eq. (12) for the inverse matrix $(s\,\mathbb{1} - \Upsilon)^{-1} = \mathrm{adj}\,(s\,\mathbb{1} - \Upsilon)/p(s)$ gives

$$\begin{aligned} p(s)\,\mathbb{1} &= (s\,\mathbb{1} - \Upsilon)\,\mathrm{adj}\,(s\,\mathbb{1} - \Upsilon) \\ &= s\sum_{j=0}^{2} p_j(s)\Upsilon^j - \Upsilon\sum_{j=0}^{2} p_j(\Upsilon)s^j. \end{aligned} \qquad \text{(A2)}$$

For the $j = 0$ term, make the substitution $s\,p_0(s)\,\mathbb{1} = [\,p(s) - c_0\,]\,\mathbb{1}$ using Eq. (31). Similarly, $\Upsilon\,p_0(\Upsilon) = p(\Upsilon) - c_0\,\mathbb{1}$. But $p(\Upsilon) = 0$ from the Cayley-Hamilton theorem, and we are left with $p(s)$ on both sides of the equation plus the remaining sum, which is easily shown to equal zero upon evaluating $p_1(x) = c_2 + x^2$ and $p_2(x) = 1$ for $x = s$ and $x = \Upsilon$.

Appendix B: An Alternative Method for Calculating an Eigenvector

Equation (A2) suggests the modest result, at the least not widely recognized, that an eigenvector $\boldsymbol{\upsilon}$ corresponding to a distinct eigenvalue υ of operator Υ can be obtained as

$$\boldsymbol{\upsilon} \in \mathrm{adj}\,(\upsilon\mathbb{1} - \Upsilon), \qquad \text{(B1)}$$

seen as follows. The characteristic polynomial $p(s)$ equals zero for eigenvalue $s = \upsilon$. Then

$$\begin{aligned} p(s) &= (s\mathbb{1} - \Upsilon)\,\mathrm{adj}\,(s\mathbb{1} - \Upsilon) \\ 0 &= (\upsilon\mathbb{1} - \Upsilon)\,\mathrm{adj}\,(\upsilon\mathbb{1} - \Upsilon) \\ \therefore \quad \Upsilon\,\mathrm{adj}\,(\upsilon\mathbb{1} - \Upsilon) &= \upsilon\,\mathrm{adj}\,(\upsilon\mathbb{1} - \Upsilon) \end{aligned} \qquad \text{(B2)}$$

Only a single column of the adjugate matrix is required, so the method is fairly efficient. However, the trivial zero eigenvector solution can be one of the columns, requiring further completion of the adjugate to obtain the desired eigenvector.

For the case of degenerate eigenvalues, the method is incomplete. When the nullity (dimension of the null space) of $(\upsilon\mathbb{1} - \Upsilon)$ equals the order of the degeneracy, k (i.e, the rank equals the dimension of the operator, n, minus k), there are k distinct eigenvectors, but the method fails, returning only the zero eigenvector. If there is not a complete set of eigenvectors (the degenerate eigenvalue is defective in that the nullity is less than k), and the rank is greater than $(n-k)$, the method appears to return the eigenvectors that exist, but one rarely needs these, since the matrix Υ is not diagonalizable in this case.

Appendix C: Cubic Polynomials with Real Coefficients

The standard solutions for the three roots of Eq. (19), cast here in terms of

$$\Lambda_\pm = \left[\, -\tilde{c}_0/\,2 \pm \sqrt{(\tilde{c}_0/2)^2 + (\tilde{c}_1/3)^3}\,\right]^{1/3}, \qquad \text{(C1)}$$

are

$$\begin{aligned} z &= \left\{\Lambda_+ + \Lambda_-, -\frac{\Lambda_+ + \Lambda_-}{2} \pm \sqrt{-3}\,\frac{\Lambda_+ - \Lambda_-}{2}\right\}, \\ &= \{z_1, z_\pm\}. \end{aligned} \qquad \text{(C2)}$$

These solutions can be consolidated in a convenient form that does not appear to have been employed heretofore. Substituting $(\Lambda_+ - \Lambda_-) = \left[(\Lambda_+ + \Lambda_-)^2 - 4\Lambda_+\Lambda_-\right]^{1/2}$ and noting $\Lambda_+\Lambda_- = -\tilde{c}_1/3$ gives

$$\begin{aligned} z_1 &= \Lambda_+ + \Lambda_- \\ z_\pm &= -\frac{1}{2}z_1 \,\pm\, i\sqrt{3}\sqrt{\left(\frac{z_1}{2}\right)^2 + \frac{\tilde{c}_1}{3}} \\ &= -\frac{1}{2}z_1 \,\pm\, i\,\varpi \end{aligned} \qquad \text{(C3)}$$

in terms of a discriminant

$$\varpi^2 = 3\left[(z_1/2)^2 + \tilde{c}_1/3\right]. \qquad \text{(C4)}$$

Any polynomial with real coefficients has at least one real root. Therefore $\varpi^2 > 0$ gives one real and two complex conjugate roots, with three real roots resulting from $\varpi^2 \leq 0$.

One can then employ simple forms for z_1 [37, 38]. The number of conditional dependencies relating z_1 in the cited references to the signs and relative magnitudes of $\tilde{c}_1$ and $\tilde{c}_0$ are simplified here in terms of

$$\begin{aligned} \alpha &= |\,\tilde{c}_1/3\,| \\ \beta &= |\,\tilde{c}_0/2\,| \\ \gamma &= \frac{\beta}{\alpha^{3/2}}. \end{aligned} \qquad \text{(C5)}$$

Then the roots can be calculated according to their domain of applicability as

$$
\begin{aligned}
&\tilde{c}_1 > 0 \\
&\qquad \varphi \equiv \tfrac{1}{3}\sinh^{-1}\gamma \\
&\qquad x_1 \equiv \mathrm{sgn}(\tilde{c}_0)\sinh\varphi \\
&\qquad z_1 = -2\sqrt{\alpha}\,x_1 && \text{(C6a)} \\
&\qquad\quad \varpi = \sqrt{3\alpha(x_1^2+1)} = \sqrt{3\alpha}\cosh\varphi \\
&\qquad z_\pm = \sqrt{\alpha}x_1 \pm i\,\varpi \\
&\tilde{c}_1 < 0 \\
&\quad \gamma \geq 1 \\
&\qquad \varphi \equiv \tfrac{1}{3}\cosh^{-1}\gamma \\
&\qquad x_1 \equiv \mathrm{sgn}(\tilde{c}_0)\cosh\varphi \\
&\qquad z_1 = -2\sqrt{\alpha}x_1 && \text{(C6b)} \\
&\qquad\quad \varpi = \sqrt{3\alpha(x_1^2-1)} = \sqrt{3\alpha}\sinh\varphi \\
&\qquad z_\pm = \sqrt{\alpha}x_1 \pm i\,\varpi \\
&\qquad\quad \to \sqrt{\alpha}x_1 \qquad \gamma = 1 \\
&\quad \gamma \leq 1 \\
&\qquad \varphi \equiv \tfrac{1}{3}\cos^{-1}\gamma \\
&\qquad x_1 \equiv \mathrm{sgn}(\tilde{c}_0)\cos\varphi \\
&\qquad z_1 = -2\sqrt{\alpha}\,x_1 && \text{(C6c)} \\
&\qquad\quad \varpi = i\sqrt{3\alpha(1-x_1^2)} = i\sqrt{3\alpha}\sin\varphi \\
&\qquad\qquad = i\,\mu \\
&\qquad z_\pm = \sqrt{\alpha}x_1 \pm \mu \qquad \text{or, alternatively} \\
&\qquad \varphi \equiv \tfrac{1}{3}\sin^{-1}\gamma \\
&\qquad x_1 \equiv \mathrm{sgn}(\tilde{c}_0)\sin\varphi \\
&\qquad z_1 = +2\sqrt{\alpha}\,x_1 && \text{(C6d)} \\
&\qquad\quad \varpi = i\sqrt{3\alpha(1-x_1^2)} = i\sqrt{3\alpha}\cos\varphi \\
&\qquad\qquad = i\,\mu \\
&\qquad z_\pm = -\sqrt{\alpha}x_1 \pm \mu \\
&\tilde{c}_1 = 0 \\
&\qquad z_1 = -\mathrm{sgn}(\tilde{c}_0)\sqrt[3]{|b|} && \text{(C6e)} \\
&\qquad z_\pm = -\frac{1}{2}z_1(1 \pm i\sqrt{3})
\end{aligned}
$$

For ($\tilde{c}_1 > 0$) or ($\tilde{c}_1 < 0$ and $\gamma > 1$), there is one real root and complex conjugate roots $z_\pm$. For $\tilde{c}_1 < 0$, $\gamma < 1$, there are three real roots. When $\gamma = 1$, both Eq. (C6b) and Eq. (C6c) give $\varphi = 0 = \varpi$ and two degenerate roots $z_+ = z_-$. Equation (C6d) reorders the roots relative to Eq. (C6c), so that the nondegenerate root for the case $\gamma = 1$ is one of the $z_\pm$. Results for $\tilde{c}_1 = 0$ are straightforwardly obtained from Eq. (C2) and Eq. (21), or using the expressions in (C6a) and (C6b), with $\sinh^{-1}\gamma \to \cosh^{-1}\gamma \to \ln(2\gamma)$ in the limit $\gamma \to \infty$. Terms then result that are multiplied by $\sqrt{\alpha}$, canceling the singularity at $\tilde{c}_1 = 0$. For the case $\tilde{c}_1 = 0 = \tilde{c}_0$, there are three equal roots $z_i = 0$.

Appendix D: Calculation of $e^{-\Gamma_\mathbf{P} t}$

1. First-order pole

Consider the case of one real root z_1 and two complex conjugate roots $z_{2,3} = -1/2z_1 \pm i\,\varpi$, as given by Eq. (21), with $\varpi^2 = 3(z_1/2)^2 + \tilde{c}_1 > 0$. Two of the terms in Eq. (35) for the Cayley-Hamilton coefficients $a_j(t)$ are therefore also complex conjugates of each other, of the form $w + w^* = 2\,\mathrm{Re}(w)$ for the sum of w and its complex conjugate. Then

$$a_j(t) = \frac{q_j(z_1)}{q'(z_1)}e^{z_1 t} + 2\,\mathrm{Re}\left[\frac{q_j(z_2)}{q'(z_2)}e^{z_2 t}\right], \qquad \text{(D1)}$$

with $q'(z_i) = \prod_{j \neq i}(z_i - z_j)$, as discussed in section III D. Evaluating the $q'(z_i)$ and using Eq. (22) for ϖ^2 gives

$$
\begin{aligned}
q'(z_1) &= (z_1 - z_2)(z_1 - z_3) \\
&= (3/2z_1)^2 + \varpi^2 \\
&= 3z_1^2 + \tilde{c}_1,
\end{aligned}
$$

$$
\begin{aligned}
q'(z_2) &= (z_2 - z_1)(z_2 - z_3) \\
&= -q'(z_1)(z_2 - z_3)/(z_1 - z_3) \\
&= -\,(3z_1^2 + \tilde{c}_1)\,2i\varpi/(3/2\,z_1 + i\,\varpi). \qquad \text{(D2)}
\end{aligned}
$$

The $q_j(z)$ are defined in Eq. (31), giving

$$q_0(z) = \tilde{c}_1 + z^2 \qquad q_1(z) = z \qquad q_2(z) = 1 \qquad \text{(D3)}$$

for a cubic polynomial in the standard canonical form of Eq. (19). Evaluating Eq. (D1) gives

$$
\begin{aligned}
a_0 &\sim e^{z_1 t}\,(z_1^2 + \tilde{c}_1) + e^{-z_1 t/2}\left[2z_1^2\cos\varpi t - \tilde{c}_1 z_1\frac{\sin\varpi\,t}{\varpi}\right] \\
a_1 &\sim z_1 e^{z_1 t} + e^{-z_1 t/2}\left[-\,z_1\cos\varpi t + (\tfrac{3}{2}z_1^2 + \tilde{c}_1)\frac{\sin\varpi t}{\varpi}\right] \\
a_2 &\sim e^{z_1 t} - e^{-z_1 t/2}\left[\cos\varpi t + \tfrac{3}{2}z_1\frac{\sin\varpi t}{\varpi}\right], \qquad \text{(D4)}
\end{aligned}
$$

with a common factor $(3z_1^2 + \tilde{c}_1)^{-1}$ multiplying each $a_i(t)$.

Arranging coefficients of each time-dependent term in a matrix gives the result in Eq. (37). All three roots are real when $\varpi^2 < 0$, which is the case for $\tilde{c}_1 < 0$ and $\gamma < 1$. Then $\varpi \to i\mu$ in Eq. (37), with $\mu^2 = |3(z_1^2/2) + \tilde{c}_1|$ and $\tilde{c}_1 = -|\tilde{c}_1|$.

2. Second-order pole

The case $\varpi = 0$ resulting from $\tilde{c}_1 = -3(z_1/2)^2$ in Eq. (22) gives doubly-degenerate real roots $z_2 = z_3 = -z_1/2$ and $q(z) \to (z - z_1)(z - z_2)^2$. The residue at $z = z_2$ in Eq. (29) for the Cayley-Hamilton coefficients $a_j(t)$ requires the derivative of $e^{zt}q_j(z)/(z - z_1)$ with respect to z, evaluated at $z = z_2$. Calculating the residue according to Eq. (16) and substituting $z_2 = -z_1/2$ gives

$$a_0(t) = e^{-z_1 t/2}\left(\frac{8}{9} + \frac{1}{3} z_1 t\right)$$

$$a_1(t) = e^{-z_1 t/2}\left(-\frac{4}{9}\, z_1^{-1} + \frac{1}{3}\, t\right)$$

$$a_2(t) = -e^{-z_1 t/2}\left(\frac{4}{9}\, z_1^{-2} + \frac{2}{3}\, t\, z_1^{-1}\right) \tag{D5}$$

The contribution from the first-order pole at z_1 is obtained as before from the simple-pole term of Eq. (37), i.e., the first column of $W_1(z_1)$ and the first element of $u_1(t)$ remain the same.

3. Third-order pole

When $\tilde{c}_0 = 0 = \tilde{c}_1$, the characteristic polynomial $q\,(z) \to z^3$, with a triply degenerate, real root $z_1 = 0$. The residue at $z = 0$ in Eq. (29) for the Cayley-Hamilton coefficients $a_j(t)$ is one-half the second derivative of $q_j(z)\, e^{zt}$ with respect to z, evaluated at $z = 0$, giving

$$a_j(t) = \left[\frac{1}{2}\, q_j''(z) + t\, q_j'(z) + \frac{1}{2}\, t^2 q(z)\right] e^{zt}\Bigg|_{z=0}$$

$$a_0(t) = 1 \qquad a_1(t) = t \qquad a_2(t) = \frac{1}{2} t^2\,. \tag{D6}$$

Appendix E: Existence of Degenerate Roots

The characteristic polynomial for the case $R_1 = R_2$ has degenerate roots for $D(\tilde{c}_0, \tilde{c}_1) = 0$ [see Eq. (46)], which requires $\tilde{c}_1 < 0$. The special case $\tilde{c}_0 = 0 = \tilde{c}_1$ discussed in section IV A gives $\omega_3^2 = 1$ and $\omega_{12}^2 = 8$, normalized to $R_\delta^2/3$. More generally, scale ω_3^2 and ω_{12}^2 in terms of the same normalization as

$$\omega_3^2 = \lambda_3\, R_\delta^2/3, \tag{E1}$$

where $\lambda_3 \geq 0$, and

$$\omega_{12}^2 = (\eta - \lambda_3 + 9/4)\, R_\delta^2/3. \tag{E2}$$

Then $D(\tilde{c}_0, \tilde{c}_1) = 0$ gives

$$\eta^3 + a_\eta \eta + b_\eta = 0, \tag{E3}$$

with

$$\frac{a_\eta}{3} = -\left(\frac{3}{2}\right)^4 (8\lambda_3 + 1)$$

$$\frac{b_\eta}{2} = \left(\frac{3}{2}\right)^6 (8\lambda_3^2 + 20\lambda_3 - 1). \tag{E4}$$

The roots $\eta_1(\lambda_3)$ and $\eta_\pm(\lambda_3)$ of Eq. (E3) can then be obtained using Eqs. (C6) with the appropriate substitution of variables. Only those solutions such that $\omega_{12}^2 \geq 0$ (i.e., is real) are of interest. The results, outlined in detail below, are that (i) there are no degenerate roots if $\omega_3^2 > R_\delta^2/3$; and (ii) for each ω_3 satisfying $0 \leq \omega_3^2 \leq R_\delta^2/3$, there are two values of ω_{12}^2 that give degenerate roots.

Note for use in what follows that

· $a_\eta < 0$ for all $\lambda_3 \geq 0$

  $\therefore$ no Eq. (C6a) solutions for η

· $\sqrt{\alpha_\eta} = \sqrt{|a_\eta/3|} = \frac{9}{4}\sqrt{8\lambda_3 + 1}$

· $b_\eta = 0$ for $\lambda_3 = \frac{3}{4}(\sqrt{3} - \frac{5}{3}) \equiv \lambda_b \approx 0.05$

· $D(a_\eta, b_\eta) = \dfrac{3^{12}}{2^6}\, \lambda_3\, (\lambda_3 - 1)^3$

· $\gamma_\eta(\lambda_3) = \dfrac{|8\lambda_3^2 + 20\lambda_3 - 1|}{(8\lambda_3 + 1)^{3/2}}$ [see Eq. (C5)]

  $\gamma_\eta(0) = 1, \quad \gamma_\eta(\lambda_b) = 0, \quad \gamma_\eta(1) = 1$

1) If $\lambda_3 > 1$, then

  · $D(a_\eta, b_\eta) > 0$, equivalent to $\gamma_\eta > 1$
  · there is one real solution η_1 from Eq. (C6b)
  · Define $\varphi_\eta = \frac{1}{3}\cosh^{-1}\gamma_\eta$
  · $b_\eta > 0$

  · $\eta_1 = -2\sqrt{\alpha_\eta}\cosh\varphi_\eta$

   $\cosh\varphi_\eta \geq 1$ for all φ_η,
   $2\sqrt{\alpha_\eta} > \frac{9}{2}\,(3)$

  $\therefore \eta_1 < -\frac{27}{2}$
  $\implies \omega_{12}^2 \sim (\eta_1 + \frac{9}{4} - \lambda_3) < -\frac{45}{4} - \lambda_3 < 0$

- No real ω_{12} such that Eq. (19) has degenerate roots for $\omega_3^2 = \lambda_3\, R_\delta^2/3 > R_\delta^2/3$

2) If $\lambda_3 \leq 1$, then

  · $\omega_{12}^2 \sim (\eta + \frac{9}{4} - \lambda_3) \geq 0$ for $\eta \geq 0$
  · $D(a_\eta, b_\eta) \leq 0$, equivalent to $\gamma_\eta \leq 1$
  · there are three real solutions $\eta_1, \eta_\pm$ from Eq. (C6d)
  · Define $\vartheta = \frac{1}{3}\sin^{-1}(\gamma_\eta)$

 (a) If $\lambda_b \leq \lambda_3 \leq 1$, then
   $0 \leq \gamma_\eta \leq 1$,
   $0 \leq \vartheta \leq \pi/6$,
   $b_\eta \geq 0$

  · $\eta_1 = 2\sqrt{\alpha_\eta}\sin\vartheta$
   $\therefore \quad \eta_1 \geq 0$
   $\implies \omega_{12}^2 > 0$

  · $\eta_\pm = -\sqrt{\alpha_\eta}\,\sin\vartheta \pm \sqrt{3}\,(\alpha_\eta - \alpha_\eta \sin^2\vartheta)^{1/2}$
   $= \pm 2\sqrt{\alpha_\eta}\,\sin(\pi/3 \mp \vartheta)$
   $\therefore \quad \eta_+ \geq 0$
   $\implies \omega_{12}^2 > 0$

 (b) If $0 \leq \lambda_3 \leq \lambda_b$, then
   $1 \geq \gamma_\eta \geq 0$,
   $\pi/6 \geq \vartheta \geq 0$,
   $b_\eta \leq 0$

  · $\eta_1 = -2\sqrt{\alpha_\eta}\sin\vartheta$
   $\therefore\ -\frac{9}{4} \leq \eta_1 \leq 0$
   $\implies \omega_{12}^2 \sim \eta_1 + \frac{9}{4} - \lambda_3 \geq 0$,
    since $\eta_1 \in [-\frac{9}{4}, 0\,]$ as $\lambda_3 \in [0, \lambda_b]$

  · $\eta_\pm = \sqrt{\alpha_\eta}\,\sin\vartheta \pm \sqrt{3}\,(\alpha_\eta - \alpha_\eta \sin^2\vartheta)^{1/2}$
   $= 2\sqrt{\alpha_\eta}\,\sin(\vartheta \pm \pi/3)$

$$\therefore \eta_+ \geq 0$$
$$\implies \omega_{12}^2 > 0$$

- 2 real ω_{12}^2 such that Eq. (19) has degenerate roots for $0 \leq \omega_3^2 \leq R_\delta^2/3$

The solutions for ω_{12}^2 become equal at $\omega_3^2 = R_\delta^2/3$, as shown in Fig. 1, corresponding to the case $\tilde{c}_1 = 0 = \tilde{c}_0$. There is then a three-fold degenerate root $z = 0$ of Eq. (19). Recall that a solution to $D(\tilde{c}_0, \tilde{c}_1) = 0$ for real $\tilde{c}_0, \tilde{c}_1$ requires $\tilde{c}_1 = \omega_{12}^2 + \omega_3^2 - 3R_\delta^2 \leq 0$, which is readily verified for the solutions obtained above. Scaling $\tilde{c}_1$ according to Eq. (E1) and Eq. (E2), dividing by $R_\delta^2/3$, and using the maximum value $\eta_{\max} = \sqrt{\alpha_\eta} = 27/4$ at $\lambda_3 = 1$ gives

$$\begin{aligned} \tilde{c}_1 &\sim (\eta - \lambda_3 + \tfrac{9}{4}) + \lambda_3 - 9 \\ &\leq \tfrac{27}{4} + \tfrac{9}{4} - 9 = 0. \end{aligned} \tag{E5}$$

Appendix F: Vector Model

There is a simple physical interpretation for the action of the propagator $e^{-\Gamma t}$ when, as is most common, the matrix Γ has three distinct eigenvalues. Supplementary details of the model introduced in section V C are presented here. Consider the case of one real eigenvalue and two complex conjugate eigenvalues. Results for the other possibility, that of three real eigenvalues, are obtained directly from Eq. (F5) in what follows.

The eigenvalues of $-\Gamma$ are the roots $s_1 = z_1 - \bar{R}$ and $s_{2,3} \equiv s_\pm = -z_1/2 \pm i\,\varpi - \bar{R}$, obtained from Eq. (24), with real z_1 given in Eqs. (C6). The associated eigenvectors are $\boldsymbol{s}_1$ and the complex conjugate pair $\boldsymbol{s}_\pm$. The relation between $\boldsymbol{s}_\pm$ and the real vectors $\tilde{\boldsymbol{s}}_2$ and $\tilde{\boldsymbol{s}}_3$ defined in Eq. (60) is

$$\begin{aligned} \tilde{\boldsymbol{s}}_2 &= \tfrac{1}{2}\,(\boldsymbol{s}_+ + \boldsymbol{s}_-) \qquad & \tilde{\boldsymbol{s}}_3 &= -\tfrac{i}{2}\,(\boldsymbol{s}_+ - \boldsymbol{s}_-) \\ \boldsymbol{s}_+ &= \tilde{\boldsymbol{s}}_2 + i\,\tilde{\boldsymbol{s}}_3 \qquad & \boldsymbol{s}_- &= \tilde{\boldsymbol{s}}_2 - i\,\tilde{\boldsymbol{s}}_3\,. \end{aligned} \tag{F1}$$

Defining $\tilde{\boldsymbol{s}}_1 \equiv \boldsymbol{s}_1$ gives a set $\tilde{\boldsymbol{s}}_i$ of three linearly independent vectors that can be used as an alternative basis for representing arbitrary system states. We then have

$$-\Gamma\,\tilde{\boldsymbol{s}}_2 = \tfrac{1}{2}\,(s_+\boldsymbol{s}_+ + s_-\boldsymbol{s}_-) = \tfrac{1}{2}\,(s_+\boldsymbol{s}_+ + s_+^*\boldsymbol{s}_+^*)$$

$$\begin{aligned} e^{-\Gamma t}\,\tilde{\boldsymbol{s}}_2 &= \tfrac{1}{2}\,(e^{s_+ t}\boldsymbol{s}_+ + e^{s_+^* t}\boldsymbol{s}_+^*) = \mathrm{Re}\,[\,e^{s_+ t}\boldsymbol{s}_+\,] \\ &= e^{-(\bar{R}+z_1/2)\,t}\,\mathrm{Re}\,[\,e^{i\varpi t}(\tilde{\boldsymbol{s}}_2 + i\,\tilde{\boldsymbol{s}}_3)\,] \\ &= e^{-(\bar{R}+z_1/2)\,t}\,(\,\cos\varpi t\,\tilde{\boldsymbol{s}}_2 - \sin\varpi t\,\tilde{\boldsymbol{s}}_3\,)\,. \end{aligned} \tag{F2}$$

Similarly,

$$\begin{aligned} e^{-\Gamma t}\,\tilde{\boldsymbol{s}}_3 &= -\tfrac{i}{2}\,(e^{s_+ t}\boldsymbol{s}_+ - e^{s_+^* t}\boldsymbol{s}_+^*) = \mathrm{Im}\,[\,e^{s_+ t}\boldsymbol{s}_+\,] \\ &= e^{-(\bar{R}+z_1/2)\,t}\,\mathrm{Im}\,[\,e^{i\varpi t}(\tilde{\boldsymbol{s}}_2 + i\,\tilde{\boldsymbol{s}}_3)\,] \\ &= e^{-(\bar{R}+z_1/2)\,t}\,(\,\sin\varpi t\,\tilde{\boldsymbol{s}}_2 + \cos\varpi t\,\tilde{\boldsymbol{s}}_3\,)\,. \end{aligned} \tag{F3}$$

These relations, together with $e^{-\Gamma\,t}\tilde{\boldsymbol{s}}_1 = e^{s_1}\tilde{\boldsymbol{s}}_1$, yield the propagator $e^{-\tilde{\Gamma}\,t}$ for the evolution of states $\tilde{\mathcal{M}} = \sum_i \tilde{\mathcal{M}}_i \tilde{\boldsymbol{s}}_i$ expressed in the $\{\tilde{\boldsymbol{s}}_i\}$ basis, as given in Eq. (63).

As noted in Eq. (61), matrix P generated from the $\{\tilde{\boldsymbol{s}}_i\}$ entered as column vectors transforms from the $\{\tilde{\boldsymbol{s}}_i\}$ basis to the standard basis, with $P^{-1} = \mathrm{adj}\,P/\det P$ giving the desired $\tilde{\mathcal{M}}$ starting with $\mathcal{M}$ in the standard basis. One easily shows that $\det P = \tilde{\boldsymbol{s}}_1 \cdot (\tilde{\boldsymbol{s}}_2 \times \tilde{\boldsymbol{s}}_3)$, and row i, column l of $\mathrm{adj}\,P$ is $(\tilde{\boldsymbol{s}}_j \times \tilde{\boldsymbol{s}}_k)_l$ for cyclic permutation of $i = 1, j = 2,$ and $k = 3$ to obtain

$$P^{-1} = \frac{1}{\tilde{\boldsymbol{s}}_1 \cdot (\tilde{\boldsymbol{s}}_2 \times \tilde{\boldsymbol{s}}_3)} \begin{bmatrix} \cdots & (\tilde{\boldsymbol{s}}_2 \times \tilde{\boldsymbol{s}}_3) & \cdots \\ \cdots & (\tilde{\boldsymbol{s}}_3 \times \tilde{\boldsymbol{s}}_1) & \cdots \\ \cdots & (\tilde{\boldsymbol{s}}_1 \times \tilde{\boldsymbol{s}}_2) & \cdots \end{bmatrix} \tag{F4}$$

The eigenvectors needed to construct the real basis are most readily obtained as any column of $\mathrm{adj}\,A(s_i) = \mathrm{adj}\,(s_i\mathbb{1} + \Gamma)$ for each eigenvalue s_i (see Appendix B). Performing the straightforward calculation gives the following result for the eigenvectors, with the left arrow signifying that the columns of the matrix map to $\boldsymbol{s}_i$:

$$\begin{aligned} \boldsymbol{s}_i \leftarrow \mathrm{adj}\,A(s_i) \;&=\; \begin{bmatrix} -\Gamma_{23}\Gamma_{32} + (s_i+R_2)(s_i+R_3) & \Gamma_{13}\Gamma_{32} - \Gamma_{12}(s_i+R_3) & \Gamma_{12}\Gamma_{23} - \Gamma_{13}(s_i+R_2) \\ \Gamma_{31}\Gamma_{23} - \Gamma_{21}(s_i+R_3) & -\Gamma_{13}\Gamma_{31} + (s_i+R_1)(s_i+R_3) & \Gamma_{13}\Gamma_{21} - \Gamma_{23}(s_i+R_1) \\ \Gamma_{21}\Gamma_{32} - \Gamma_{31}(s_i+R_2) & \Gamma_{31}\Gamma_{12} - \Gamma_{32}(s_i+R_1) & -\Gamma_{12}\Gamma_{21} + (s_i+R_1)(s_i+R_2) \end{bmatrix} \\ &\xrightarrow{\text{OBE}} \begin{bmatrix} \omega_1^2 + (s_i+R_2)(s_i+R_3) & \omega_1\omega_2 - \omega_3(s_i+R_3) & \omega_1\omega_3 + \omega_2(s_i+R_2) \\ \omega_1\omega_2 + \omega_3(s_i+R_3) & \omega_2^2 + (s_i+R_1)(s_i+R_3) & \omega_2\omega_3 - \omega_1(s_i+R_1) \\ \omega_1\omega_3 - \omega_2(s_i+R_2) & \omega_2\omega_3 + \omega_1(s_i+R_1) & \omega_3^2 + (s_i+R_1)(s_i+R_2) \end{bmatrix}. \end{aligned} \tag{F5}$$

The three different forms of a given $\boldsymbol{s}_i$ are therefore related by a scale factor, despite perhaps appearing otherwise. The scaling can be verified by calculating the eigenvectors in the usual fashion as solutions to $(s_i\mathbb{1} + \Gamma)\boldsymbol{s}_i = 0$. This system of equations is overdetermined, by construction, so any one of the three equations is a linear combination of the other two and is redundant. We are free to assign any (nonzero) value to one of the components, leaving two equations and two unknowns. There are three different but equivalent forms for the eigenvector solution depending on which two equations are chosen. Setting the third component equal to one gives an expression for the other two components involving a common denominator. Scaling each eigenvector by the denominator of its other two components gives the result in Eq. (F5).

For the OBE in the absence of relaxation ($R_i = 0$), Γ generates a rotation about $\boldsymbol{\omega}_e$, as is well known. The real eigenvalue of $-\Gamma$ is $s_1 = 0$ with eigenvector $\boldsymbol{s}_1 = (\omega_1, \omega_2, \omega_3)$, obtained by dividing column j of $\operatorname{adj} A(s_1)$ by (nonzero) ω_j. This is the expected rotation axis for the resulting time evolution. If $\boldsymbol{\omega}_e = 0$, then Γ is already diagonal, and the coordinates reduce to the standard coordinate system as required.

We also have $\operatorname{adj} A(s_i) = \operatorname{adj} A_{\mathrm{p}}(z_i)$, since $s_i = z_i - \bar{R}$ and $R_i - \bar{R} = R_{i\mathrm{p}}$. The real basis vectors $\tilde{\boldsymbol{s}}_{2,3} \equiv \tilde{\boldsymbol{z}}_{2,3}$ are equal to the respective real, imaginary parts of $\boldsymbol{z}_+ = \operatorname{adj} A_{\mathrm{p}}(z_+)$ according to Eq. (60), with $z_+ = -z_1/2 + i\,\varpi$. Then, using Eq. (26) for $\operatorname{adj} A_{\mathrm{p}}(z_i)$ in polynomial form and eliminating common scale factors, the real basis vectors defining the oblique coordinate system can be written concisely as

$$
\begin{aligned}
\tilde{\boldsymbol{s}}_1 &= \tilde{\boldsymbol{z}}_1 \leftarrow A_{0\mathrm{p}} + A_{1\mathrm{p}}\, z_1 + \mathbb{1}\, z_1^2 \\
\tilde{\boldsymbol{s}}_2 &= \tilde{\boldsymbol{z}}_2 \leftarrow A_{0\mathrm{p}} - A_{1\mathrm{p}}\, \frac{z_1}{2} + \mathbb{1}\left[\left(\frac{z_1}{2}\right)^2 - \varpi^2\right] \\
\tilde{\boldsymbol{s}}_3 &= \tilde{\boldsymbol{z}}_3 \leftarrow A_{1\mathrm{p}} - \mathbb{1}\, z_1
\end{aligned}
\tag{F6}
$$

The result for $\tilde{\boldsymbol{z}}_1$ can be obtained directly from Eq. (F5) with the substitutions $s_i \to z_i$ and $R_i \to R_{ip}$ for the corresponding parameters associated with Γ_{p}. One can readily deduce the coefficient matrices $A_{0\mathrm{p}}$ and $A_{1\mathrm{p}}$ by comparing Eq. (F5) with the polynomial form in Eq. (26), also given above in the expression for $\tilde{\boldsymbol{s}}_1$. Recall that $\sum_i R_{i\mathrm{p}} = 0$ by construction in the original matrix partitioning, so we can simplify terms such as $R_{2\mathrm{p}} + R_{3\mathrm{p}} \to -R_{1\mathrm{p}}$ and its cyclic permutations. The coefficients can also be obtained as simple functions of Γ_{p} using Eq. (27). For the OBE parameters, each coefficient matrix is

$$
\begin{aligned}
A_{0\mathrm{p}} &= \begin{bmatrix} \omega_1^2 + R_{2\mathrm{p}}R_{3\mathrm{p}} & \omega_1\omega_2 - \omega_3 R_{3\mathrm{p}} & \omega_1\omega_3 + \omega_2 R_{2p} \\ \omega_1\omega_2 + \omega_3 R_{3\mathrm{p}} & \omega_2^2 + R_{1\mathrm{p}}R_{3\mathrm{p}} & \omega_2\omega_3 - \omega_1 R_{1\mathrm{p}} \\ \omega_1\omega_3 - \omega_2 R_{2\mathrm{p}} & \omega_2\omega_3 + \omega_1 R_{1\mathrm{p}} & \omega_3^2 + R_{1\mathrm{p}}R_{2\mathrm{p}} \end{bmatrix} \\
A_{1\mathrm{p}} &= -\Gamma_{\mathrm{p}} = \begin{bmatrix} -R_{1\mathrm{p}} & -\omega_3 & \omega_2 \\ \omega_3 & -R_{2\mathrm{p}} & -\omega_1 \\ -\omega_2 & \omega_1 & -R_{3\mathrm{p}} \end{bmatrix},
\end{aligned}
\tag{F7}
$$

with $R_{1\mathrm{p}} = R_{2\mathrm{p}} = R_\delta$ and $R_{3\mathrm{p}} = -2R_\delta$ from Eq. (44).

1. Measures of obliquity

Bloch equation dynamics are simple in the oblique coordinates of the model, consisting of independent rotation and relaxation elements. This section provides examples that quantify the degree to which the plane of rotation is oblique to the axis $\tilde{\boldsymbol{z}}_1$ representing simple exponential decay. In what follows, the first column of $\operatorname{adj} A_{\mathrm{p}}$ is arbitrarily chosen to calculate the coordinate basis $\{\tilde{\boldsymbol{z}}_i\}$, for $R_1 = R_2$. Similar results are obtained using any of the other columns.

a. *Off resonance,* $\boldsymbol{\omega}_e = (0, \omega_2, \omega_3)$

Off resonance, in contrast to the on-resonance example of section V C 4 b, $\tilde{\boldsymbol{z}}_1$ is neither aligned with $\boldsymbol{\omega}_e$, nor is it orthogonal to the $(\tilde{\boldsymbol{z}}_2, \tilde{\boldsymbol{z}}_3)$-plane. Calculating the $\tilde{\boldsymbol{z}}_i$ as above provides the normal to this plane, $\tilde{\boldsymbol{n}}_{23} = \tilde{\boldsymbol{z}}_2 \times \tilde{\boldsymbol{z}}_3$. Then

$$
\tilde{\boldsymbol{z}}_1 = \begin{pmatrix} (z_1 + R_\delta)(z_1 - 2R_\delta) \\ \omega_3(z_1 - 2R_\delta) \\ -\omega_2(z_1 + R_\delta) \end{pmatrix}
\tag{F8}
$$

and

$$
\tilde{\boldsymbol{n}}_{23} = \begin{pmatrix} 3\omega_2\omega_3 R_\delta \\ -\omega_2\left(\tilde{c}_1 - z_1 R_\delta + z_1^2 + R_\delta^2\right) \\ -\omega_3\left(\tilde{c}_1 + 2z_1 R_\delta + z_1^2 + 4R_\delta^2\right) \end{pmatrix}
\tag{F9}
$$

using $\varpi^2 = 3/4 z_1^2 + \tilde{c}_1$ from Eq. (22) in the expression for $\tilde{\boldsymbol{s}}_2$. Although the normal bears little resemblance to $\tilde{\boldsymbol{z}}_1$, let us scale $\tilde{\boldsymbol{z}}_1$ by $f_s = -(\tilde{\boldsymbol{n}}_{23})_1/(\tilde{\boldsymbol{z}}_1)_1$, so that the first component $(\tilde{\boldsymbol{z}}_1)_1 \to -(\tilde{\boldsymbol{n}}_{23})_1$. For the other two components, straightforward algebra gives the relation $f_s\tilde{\boldsymbol{z}}_1 - \tilde{\boldsymbol{n}}_{23} \propto q(z_1)$, the characteristic polynomial for $-\Gamma_{\mathrm{p}}$, which is zero when evaluated at its root z_1. Thus, within a scale factor or, equivalently, when both both vectors are normalized, we have

$$
\tilde{\boldsymbol{n}}_{23} = \begin{pmatrix} -(\tilde{\boldsymbol{z}}_1)_1 \\ (\tilde{\boldsymbol{z}}_1)_2 \\ (\tilde{\boldsymbol{z}}_1)_3 \end{pmatrix}.
\tag{F10}
$$

b. *Off resonance,* $\boldsymbol{\omega}_e = (\omega_1, 0, \omega_3)$

Similarly, for $\omega_2 = 0$,

$$
\tilde{\boldsymbol{z}}_1 = \begin{pmatrix} \omega_1^2 + (z_1 + R_\delta)(z_1 - 2R_\delta) \\ \omega_3(z_1 - 2R_\delta) \\ \omega_1\omega_3 \end{pmatrix}
\tag{F11}
$$

and

$$
\tilde{\boldsymbol{n}}_{23} = -\begin{pmatrix} \omega_1\omega_3 \\ \omega_1\left(z_1 + R_\delta\right) \\ \frac{1}{4}(z_1 + 4R_\delta)^2 + \varpi^2 - \omega_1^2 \end{pmatrix},
\tag{F12}
$$

Scaling $\tilde{\boldsymbol{z}}_1$ by $f_s = -(\tilde{\boldsymbol{n}}_{23})_2/(\tilde{\boldsymbol{z}}_1)_2$ gives $f_s\tilde{\boldsymbol{z}}_1 - \tilde{\boldsymbol{n}}_{23} \propto q(z_1)$ for components one and three, so that

$$
\tilde{\boldsymbol{n}}_{23} = \begin{pmatrix} (\tilde{\boldsymbol{z}}_1)_1 \\ -(\tilde{\boldsymbol{z}}_1)_2 \\ (\tilde{\boldsymbol{z}}_1)_3 \end{pmatrix}
\tag{F13}
$$

within a scale factor.

c. $\boldsymbol{\omega_1 = \omega_2 = \omega_3 \equiv \omega}$

In this case,

$$
\tilde{\boldsymbol{z}}_1 = \begin{pmatrix} \omega^2 + (z_1 + R_\delta)(z_1 - 2R_\delta) \\ \omega(\omega + z_1 - 2R_\delta) \\ -\omega(\omega + z_1 + R_\delta) \end{pmatrix}
\tag{F14}
$$

and

$$\tilde{\boldsymbol{n}}_{23} = -\begin{pmatrix} \omega(2\omega - 3R_\delta) \\ \frac{1}{4}(z_1 - 2R_\delta)^2 + \omega(z_1 + R_\delta) + \varpi^2 - \omega^2 \\ \frac{1}{4}(z_1 + 4R_\delta)^2 - \omega(z_1 + R_\delta) + \varpi^2 - \omega^2 \end{pmatrix}. \tag{F15}$$

Scaling $\tilde{\boldsymbol{z}}_1$ by $f_s = (\tilde{\boldsymbol{n}}_{23})_1/(\tilde{\boldsymbol{z}}_1)_2$ gives both $f_s(\tilde{\boldsymbol{z}}_1)_1 - (\tilde{\boldsymbol{n}}_{23})_2$ and $f_s(\tilde{\boldsymbol{z}}_1)_3 - (\tilde{\boldsymbol{n}}_{12})_3$ proportional to $q(z_1)$, so that the vectors can be scaled to satisfy

$$\tilde{\boldsymbol{n}}_{23} = \begin{pmatrix} (\tilde{\boldsymbol{z}}_1)_2 \\ (\tilde{\boldsymbol{z}}_1)_1 \\ (\tilde{\boldsymbol{z}}_1)_3 \end{pmatrix}. \tag{F16}$$

Appendix G: Solution Verification

The solutions are evaluated here for $R_1 = R_2$ using a representative set of limiting cases that are readily solved by other methods to check the solutions.

1. Three distinct roots

Three examples are presented representing the separate cases $\tilde{c}_0 = 0$ and $\tilde{c}_1 = 0$.

(i) $\tilde{c}_0 = 0$, $\tilde{c}_1 \neq 0$

According to the defining relations for $\tilde{c}_0$ and $\tilde{c}_1$ in Eq. (45), the condition $\tilde{c}_0 = 0$ implies $\omega_{12}^2 = 2R_\delta^2(1+\frac{1}{3}\lambda_3)$, using Eq. (3) for ω_e^2 and Eq. (47) for ω_3. Then

$$\tilde{c}_1 = \begin{cases} R_\delta^2(\lambda_3 - 1) & R_\delta \neq 0 \\ \omega_e^2 & R_\delta = 0 \end{cases} \tag{G1}$$

The roots of Eq. (19) are easily obtained, giving

$$z_1 = 0 \qquad\qquad \varpi = \sqrt{\tilde{c}_1}. \tag{G2}$$

There are two cases, depending on the sign of $\tilde{c}_1$.

(1) $\tilde{c}_1 > 0$

Equation 37 gives

$$e^{-\Gamma_\mathrm{p}\, t} = \mathbb{1} - \frac{\Gamma_\mathrm{p}}{\varpi}\sin\varpi t + \left(\frac{\Gamma_\mathrm{p}}{\varpi}\right)^2 (1 - \cos\varpi t). \tag{G3}$$

There is no exponential decay contribution due to this term, with the overall factor $e^{-\bar{R}t}$ in the final expression for $e^{-\Gamma t}$ providing a single system decay rate $\bar{R}$.

Example (1)

Choose $R_\delta = 0$ to obtain
$\tilde{c}_0 = 0, \quad \tilde{c}_1 = \omega_e^2, \quad \varpi = \omega_e.$

Then Eq. (G3) represents a rotation about the field $\boldsymbol{\omega}_e$.

The propagator U_R for a rotation about $\boldsymbol{\omega}_e$ is readily obtained by transforming to a coordinate system with new z-axis aligned with $\boldsymbol{\omega}_e$, rotating by angle $-\omega_e t$ about this axis, then transforming back to the original coordinates. Specifying the orientation of $\boldsymbol{\omega}_e$ in terms of polar angle θ and azimuthal angle ϕ relative to the z- and x-axes, respectively, one has $U_R = U_z(-\phi)U_y(-\theta)U_z(-\omega_e\, t)U_y(\theta)U_z(\phi)$ in terms of the elementary operators U_y and U_z for rotations about the y- and z- axes, respectively. Then U_R provides a verification of the Eq. (G3) result upon substituting $\cos\phi = \omega_1/\omega_{12}$, $\sin\phi = \omega_2/\omega_{12}$, $\cos\theta = \omega_3/\omega_e$, $\sin\theta = \omega_{12}/\omega_e$.

(2) $\tilde{c}_1 < 0$

for $\lambda_3 < 1$ gives $\varpi \to i\,\mu = i\,\sqrt{|\tilde{c}_1|}$ and

$$e^{-\Gamma_\mathrm{p}\, t} = \mathbb{1} - \frac{\Gamma_\mathrm{p}}{\mu}\sinh\mu t + \left(\frac{\Gamma_\mathrm{p}}{\mu}\right)^2 (\cosh\mu t - 1) \tag{G4}$$

Example (2)

Choose $\omega_1^2 = 2R_\delta^2$, $\omega_2 = 0$, $\lambda_3 = 0$ to obtain
$\tilde{c}_0 = 0, \quad \tilde{c}_1 = -R_\delta^2, \quad \mu = R_\delta$

Then Eq. (G4) gives

$$e^{-\Gamma_\mathrm{p}\, t} = \begin{pmatrix} e^{-R_\delta t} & 0 & 0 \\ 0 & 2 - e^{R_\delta t} & \sqrt{2}\,(1 - e^{R_\delta t}) \\ 0 & -\sqrt{2}\,(1 - e^{R_\delta t}) & 2\,e^{R_\delta t} - 1 \end{pmatrix}. \tag{G5}$$

For an independent calculation, the matrix $-\Gamma_\mathrm{p}$ can be diagonalized, with eigenvalues given by the z_i and associated real-valued eigenvectors. The simple exponential of the diagonalized matrix is then transformed back to the original basis in the standard fashion using the matrix of eigenvectors and its inverse to obtain $e^{-\Gamma_\mathrm{p}\, t}$ as given above.

(ii) $\tilde{c}_1 = 0$. $\tilde{c}_0 \neq 0$

The condition $\tilde{c}_1 = 0$ implies $\omega_e^2 = 3R_\delta^2$, leading to

$$\tilde{c}_0 = R_\delta^3(1 - \lambda_3) \tag{G6}$$

and root $z_1 = -\mathrm{sgn}(\tilde{c}_0)|\tilde{c}_0|^{1/3}$ from Eq. (C6e). For $\mathrm{sgn}(\tilde{c}_0) = \pm 1$ and the definition $\tilde{\lambda}_3 = |1 - \lambda_3|^{1/3}$, we have

$$z_1 = \mp\,\tilde{\lambda}_3 R_\delta \qquad\qquad \varpi = \frac{\sqrt{3}}{2}\,\tilde{\lambda}_3 R_\delta \tag{G7}$$

Although the form of Eq. (37) does not simplify in this case as appreciably as for $\tilde{c}_0 = 0$, both the root z_1, which determines the decay rate, and the oscillatory frequency ϖ are simple multiples of R_δ.

Example (3)

Choose $\omega_e^2 \to \omega_1^2 = 3R_\delta^2, \qquad \omega_2 = 0 = \omega_3.$

Then most off-diagonal elements of Γ_p are equal to zero, and $\tilde{\lambda}_3 = 1$ for the Eq. (G7) input parameters to Eq. (37). Defining $\kappa = (\sqrt{3}/2)R_\delta$ and combining the sums of trigonometric functions that appear on the diagonal gives the succinct form

$$e^{-\Gamma_{\rm p}\,t} = e^{\frac{1}{2}R_\delta t}\begin{pmatrix} e^{-\frac{3}{2}R_\delta t} & 0 & 0 \\ 0 & -2\sin\left(\kappa t-\frac{\pi}{6}\right) & -2\sin(\kappa t) \\ 0 & 2\sin(\kappa t) & 2\sin\left(\kappa t+\frac{\pi}{6}\right) \end{pmatrix} \tag{G8}$$

Again, the matrix $-\Gamma_{\rm p}$ is diagonalizable, providing a simple result for the matrix exponential in the eigenbasis and a straightforward means for calculating $e^{-\Gamma_p t}$ as obtained above. The associated eigenvectors are complex-valued in this case, making the algebra slightly more tedious. Alternatively, one can readily verify that $d/dt\, e^{-\Gamma_{\rm p}\,t} = -\Gamma_{\rm p}\, e^{-\Gamma_{\rm p}\,t}$.

2. Two equal roots

Degenerate roots require $\gamma = 1$. For a given $\omega_3^2 = \lambda_3 R_\delta^2/3$, with $0 \le \lambda_3 \le 1$, there are two values ω_{12}^2 that satisfy $\gamma = 1$, derived in Appendix E and discussed in Sec. IV A. Consider $\lambda_3 = 0$, on resonance, in which case Eqs. (47) and (48) give

$$\begin{aligned} (\vartheta_1, \vartheta_2) &= (\,-\pi/6\,,\, \pi/2\,) \\ (\eta_1, \eta_2) &= (\,-9/4\,,\, 9/2\,) \\ (\omega_{12,1}^2\,,\, \omega_{12,2}^2) &= (\,0\,,\, 9/4R_\delta^2\,). \end{aligned} \tag{G9}$$

(i) $\omega_{12} = 0$

Then there is only relaxation, with $\Gamma_{\rm p}$ reduced to the diagonal elements $\{R_\delta, R_\delta, -2R_\delta\}$. We have $\tilde{c}_1 = -3R_\delta^2$, $\tilde{c}_0 = -2R_\delta^3 < 0$, and

$$z_1 = 2R_\delta \qquad\qquad \varpi = 0 \tag{G10}$$

from Eq. (C6b). Equation (38) gives the expected result

$$e^{-\Gamma_P\,t} = \begin{pmatrix} e^{-R_\delta t} & 0 & 0 \\ 0 & e^{-R_\delta t} & 0 \\ 0 & 0 & e^{2R_\delta t} \end{pmatrix}. \tag{G11}$$

(ii) $\omega_{12}^2 = \frac{9}{4}R_\delta^2 \to \omega_1^2$

Then $\tilde{c}_1 = -3R_\delta^2/4 < 0$, $\tilde{c}_0 = R_\delta^3/4 > 0$, and

$$z_1 = -R_\delta, \qquad\qquad \varpi = 0, \tag{G12}$$

resulting in

$$e^{-\Gamma_{\rm p}\,t} = e^{\frac{1}{2}R_\delta t}\begin{pmatrix} e^{-\frac{3}{2}R_\delta t} & 0 & 0 \\ 0 & 1-\omega_1 t & -\omega_1 t \\ 0 & \omega_1 t & 1+\omega_1 t \end{pmatrix}. \tag{G13}$$

Verifying that $d/dt\, e^{-\Gamma_{\rm p}\,t} = -\Gamma_{\rm p}\, e^{-\Gamma_{\rm p}\,t}$ is fairly straightforward and represents the simplest test of the solution, since $\Gamma_{\rm p}$ is not diagonalizable.

3. Three equal roots

There is a three-fold degenerate root $z_i = 0$ in the case $\tilde{c}_0 = 0 = \tilde{c}_1$, since $q(z) \to z^3$. This requires $\omega_e^2 = 3R_\delta^2$ from Eq. (45), which then forces $\omega_3^2 = R_\delta^2/3$ in the expression for $\tilde{c}_0$. As noted previously, the Cayley-Hamilton theorem is simple to apply directly in this case, since $q(\Gamma_{\rm p}) = \Gamma_{\rm p}^3 = 0$. The series expansion of $e^{-\Gamma_{\rm p}\,t}$ is therefore truncated, giving the Eq. (39) result.

4. On resonance

When $\omega_3 = 0$, $\tilde{c}_0$ can be written in the form $R_\delta(\tilde{c}_1 + R_\delta^2)$ from Eq. (45), with $\tilde{c}_1 \to \omega_{12}^2 - 3R_\delta^2$. The characteristic polynomial then becomes $z^3 + R_\delta^3 + \tilde{c}_1(z + R_\delta)$, so that, by inspection,

$$z_1 = -R_\delta \qquad\qquad \varpi = \sqrt{\omega_{12}^2 - (\tfrac{3}{2}R_\delta)^2} \tag{G14}$$

The solution for $e^{-\Gamma_p\,t}$ using Eq. (37) with the above parameters yields the solution for $e^{-\Gamma\,t}$ obtained originally by Torrey [6] for $\varpi \neq 0$. As discussed above, if $\omega_{12} = 3R_\delta/2$ so that $\varpi = 0$, there is a two-fold degeneracy in the roots, giving the solution in Eq. (G13) for $e^{-\Gamma_p\,t}$.

For $\omega_{12} < 3R_\delta/2$, the sinusoidal terms become the corresponding hyperbolic functions, as noted earlier, with $\cos\varpi\, t \to \cosh\mu\, t$ and $\sin\varpi\, t/\varpi \to \sinh\mu\, t/\mu$, where now $\mu = \sqrt{(\frac{3}{2}R_\delta)^2 - \omega_{12}^2}$.

[1] F. Bloch, Phys. Rev., **70**, 460 (1946).

[2] R. P. Feynman, J. F. L. Vernon, and R. W. Hellwarth, J. Appl. Phys., **28**, 49 (1957).

[3] R. Chakrabarti and H. Rabitz, International Reviews in Physical Chemistry, **26**, 671 (2007), http://dx.doi.org/10.1080/01442350701633300.

[4] N. C. Nielsen, C. Kehlet, S. J. Glaser, and N. Khaneja, "Optimal control methods in NMR spectroscopy," in *eMagRes* (2010).

[5] D. Dong and I. R. Petersen, IET Control Theory and Applications, **4**, 2651 (2010).

[6] H. C. Torrey, Phys. Rev., **76**, 1059 (1949).

[7] P. K. Madhu and A. Kumar, J. Magn. Reson. A, **114**, 201 (1995).

[8] A. D. Bain, J. Magn. Reson., **206**, 227 (2010).

[9] A. Szabo and T. Muramoto, Phys. Rev. A, **37**, 4040 (1988).

[10] F. Bloch, Phys. Rev., **105**, 1206 (1957).

[11] K. Tomita, Prog. Theor. Phys., **19**, 541 (1958).
[12] E. Sziklas, Phys. Rev, **188**, 700 (1969).
[13] R. H. Lehmberg, Phys. Lett., **33A**, 501 (1970).
[14] E. Hanamura, J. Phys. Soc. Jpn., **52**, 2258 (1983).
[15] E. Hanamura, J. Phys. Soc. Jpn., **52**, 3678 (1983).
[16] M. Yamanoi and J. H. Eberly, Phys. Rev. Lett., **52**, 1353 (1984).
[17] M. Yamanoi and J. H. Eberly, J. Opt. Soc. Am. B, **1**, 751 (1984).
[18] J. Javanainen, Opt. Commun., **50**, 26 (1984).
[19] A. Schenzle, M. Mitsunaga, R. G. DeVoe, and R. G. Brewer, Phys. Rev. A, **30**, 325 (1984).
[20] P. A. Apanasevich, S. Ya-Kilin, A. P. Nizovtsev, and N. S. Onishchenko, Opt. Commun., **52**, 279 (1984).
[21] K. Wódkiewicz and J. H. Eberly, Phys. Rev. A, **32**, 992 (1985).
[22] P. R. Berman and R. G. Brewer, Phys. Rev. A, **32**, 2784 (1985).
[23] A. G. Redfield, Phys. Rev., **98**, 1787 (1955).
[24] R. G. DeVoe and R. G. Brewer, Phys. Rev. Lett., **50**, 1269 (1983).
[25] A. G. Yodh, J. Golub, N. W. Carlson, and T. W. Mossberg, Phys. Rev. Lett., **53**, 659 (1984).
[26] T. E. Skinner, Phys. Rev. A, **88**, 012110 (2013).
[27] J. S. Briggs and A. Eisfeld, Phys. Rev. A, **85**, 052111 (2012).
[28] R. P. Feynman, Rev. Mod. Phys., **20**, 367 (1948).
[29] L. Allen and J. H. Eberly, *Optical Resonance and Two-Level Atoms* (Wiley, New York, 1975).
[30] I. I. Rabi, N. F. Ramsey, and J. Schwinger, Rev. Mod. Phys, **26**, 167 (1954).
[31] E. C. Jaynes, Phys. Rev., **98**, 1099 (1955).
[32] J. B. Marion, *Classical Dynamics of Particles and Systems* (Academic Press, New York, 1970).
[33] U. Fano, Rev. Mod. Phys., **29**, 74 (1957).
[34] C. Moler and C. van Loan, Siam Review, **45**, 3 (2003).
[35] G. Arfken, *Mathematical Methods for Physicists* (Academic Press, New York, 1970).
[36] M. Lapert, E. Assémat, S. J. Glaser, and D. Sugny, Phys. Rev. A, **88**, 033407 (2013).
[37] R. M. Miura, Appl. Math Notes, **5**, 22 (1980).
[38] J. P. McKelvey, Am. J. Phys., **52**, 269 (1984).

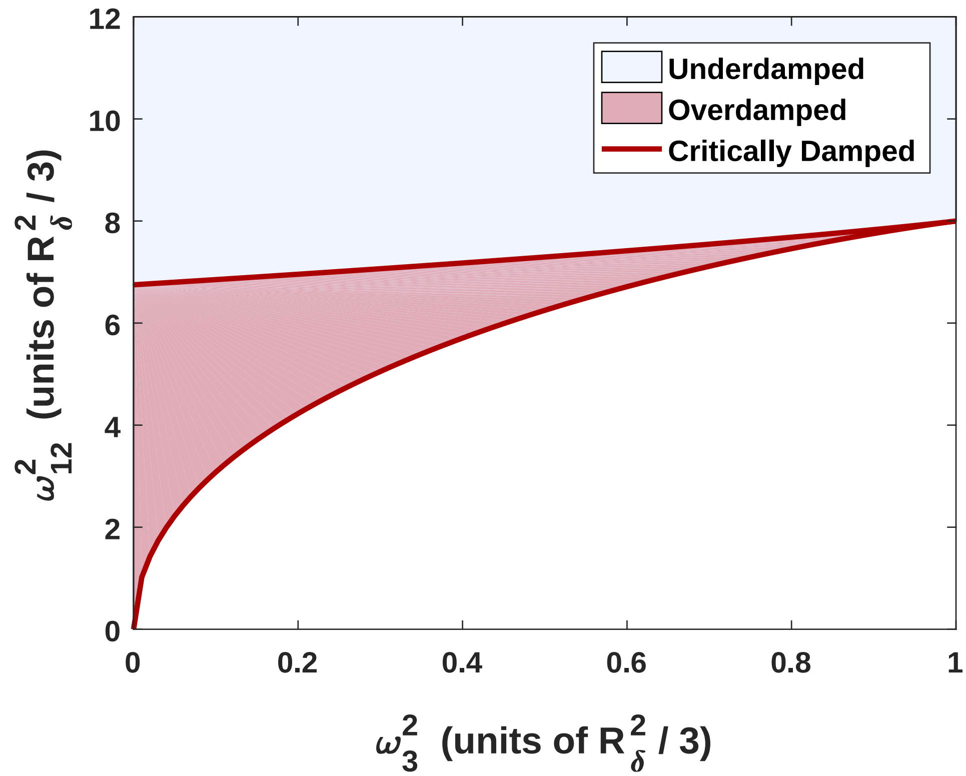

FIG. 1. Parameter values of ω_{12}^2 that give degenerate roots of the characteristic polynomial ($\gamma = 1$) and critically damped solutions to the Bloch equation are plotted as a function of ω_3^2, shown as red (solid) lines calculated using Eq. (48). The parameters are scaled to $R_\delta^2/3$ as in Eq. (47). In the interior of the region delineated by these curves (light red), there are three distinct real roots ($\tilde{c}_1 < 0\,,\ \gamma < 1$) resulting in overdamped solutions. Outside this region (light blue), one real and two complex conjugate roots produce oscillatory, underdamped solutions, with $\tilde{c}_1 > 0$ above the overdamped region and $\tilde{c}_1 > 0\,,\ \gamma > 1$ below the overdamped region.

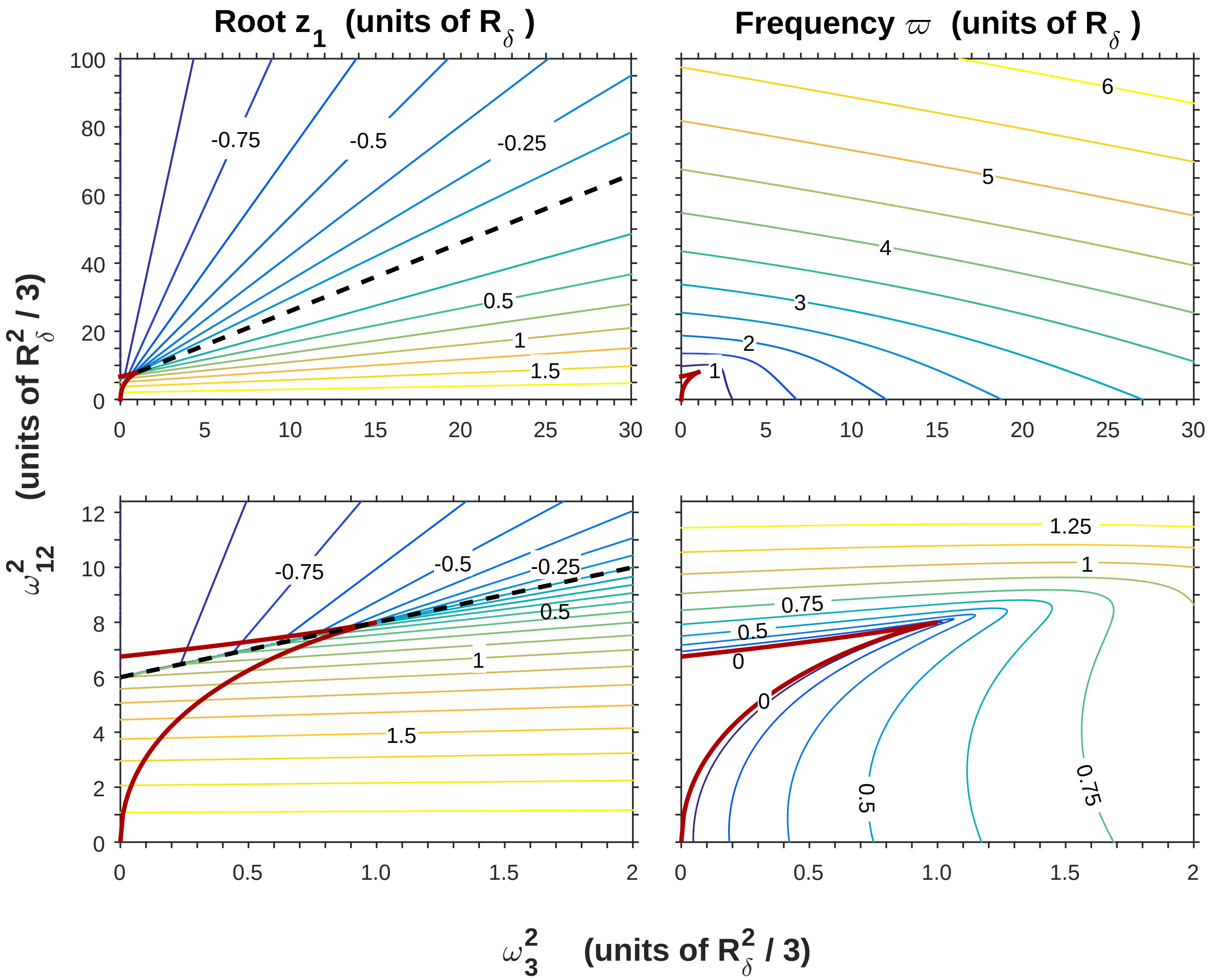

FIG. 2. Contours of the characteristic polynomial's guaranteed real root z_1, calculated according to Eqs. (C6) and normalized to R_δ, are plotted as a function of ω_{12}^2 and ω_3^2 normalized as in Fig. 1. The root satisfies $-1 \leq z_1 \leq 2$, as expected from Eq. (51), with lines of constant z_1 as derived in Eqs. (53–55). The $z_1 = 0$ contour is shown as a dashed line. Contours of the frequency ϖ from Eq. (22) that appears in the oscillatory, underdamped solutions of the Bloch equation are also plotted in the rightmost panels. Within the overdamped region defined in Fig. 1 and expanded in the lower panels, there is no oscillation or frequency ϖ, and only one of the three real roots is plotted.

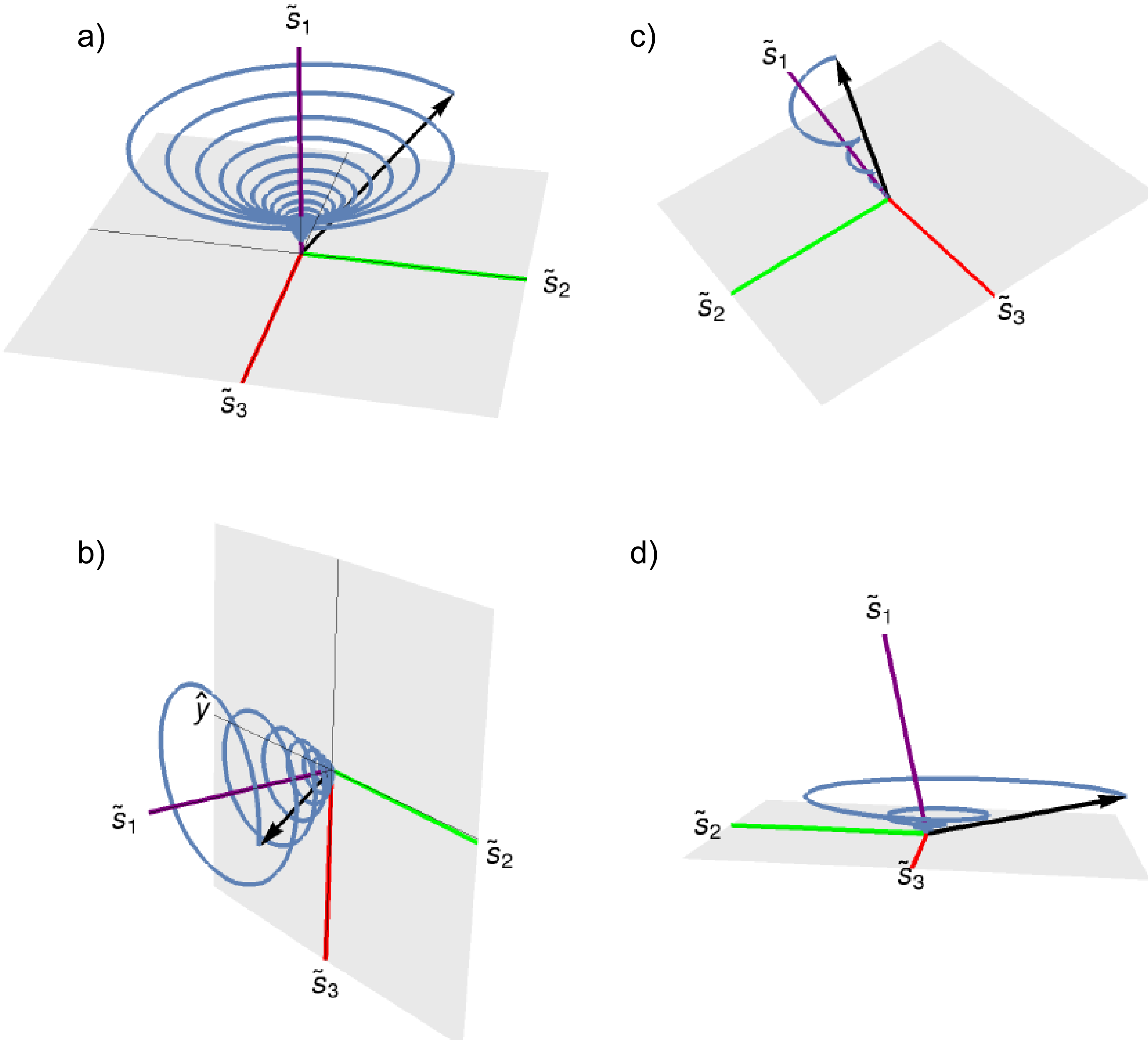

FIG. 3. Trajectories for initial vector $\mathcal{M}_0$ acted upon by propagator $e^{-\Gamma t}$ are displayed in the $\{\tilde{\boldsymbol{s}}_1, \tilde{\boldsymbol{s}}_2, \tilde{\boldsymbol{s}}_3\}$-coordinates developed as the natural system for describing propagator dynamics. The component of $\mathcal{M}_0$ along $\tilde{\boldsymbol{s}}_1$ decays at the rate $\bar{R} - z_1$, while components in the $(\tilde{\boldsymbol{s}}_2, \tilde{\boldsymbol{s}}_3)$-plane rotate in the plane and decay at the rate $\bar{R} + z_1/2$. The different panels represent different $\mathcal{M}_0$, fields $\boldsymbol{\omega}_e$, transverse relaxation rate R_2, and longitudinal relaxation rate R_3, with details of the predicted system evolution described in more detail in the text. Physical parameters are in units inverse seconds. ***(a)*** Initial state $\mathcal{M}_0 = (-1, 1, 1)$. Physical parameters $\boldsymbol{\omega}_e = (0, 0, 10^4)$, $R_2 = 400$, $R_3 = 200$ give coordinates $\tilde{\boldsymbol{s}}_1 = \hat{\boldsymbol{z}}$, $\tilde{\boldsymbol{s}}_2 = \hat{\boldsymbol{y}}$, $\tilde{\boldsymbol{s}}_3 = \hat{\boldsymbol{x}}$ and the well-known rotation about $\boldsymbol{\omega}_e = \omega_3$ followed by longitudinal and transverse relaxation. ***(b)*** Initial state $\mathcal{M}_0 = (1, -1, 0)$. Parameters $\boldsymbol{\omega}_e = (5000, 0, 0)$, $R_2 = 400$, $R_3 = 200$ lead to coordinates $\tilde{\boldsymbol{s}}_1 = \hat{\boldsymbol{x}}$, $\tilde{\boldsymbol{s}}_2 = (0, -1, .02)$, $\tilde{\boldsymbol{s}}_3 = \hat{\boldsymbol{z}}$. Rotation is also about $\boldsymbol{\omega}_e$ for $\omega_3 = 0$ (on resonance), but now $\tilde{\boldsymbol{s}}_2$ is not perpendicular to $\tilde{\boldsymbol{s}}_3$, so the rotation in the plane transverse to $\tilde{\boldsymbol{s}}_1$ is not at constant angular frequency. ***(c)*** Parameters $\boldsymbol{\omega}_e = (0, 300, 300)$, $R_2 = 100$, $R_3 = 1$ lead to non-orthogonal oblique coordinates $\tilde{\boldsymbol{s}}_1 = (0.12, 0.69, 0, 71)$, $\tilde{\boldsymbol{s}}_2 = (0.99, 0.04, 0.12)$, $\tilde{\boldsymbol{s}}_3 = (0., 0.72, -0.70)$. Initial $\mathcal{M}_0 = (-0.12, 0.69, 0, 71)$ is normal to the $(\tilde{\boldsymbol{s}}_2, \tilde{\boldsymbol{s}}_3)$-plane, but has components in the plane and along $\tilde{\boldsymbol{s}}_1$ in the oblique coordinate system, so spirals about $\tilde{\boldsymbol{s}}_1$ as shown. ***(d)*** Initial $\mathcal{M} = (-0.99, 0.17, 0)$ is orthogonal to $\tilde{\boldsymbol{s}}_1$. Parameters $\boldsymbol{\omega}_e = (0, 3000, 3000)$, $R_2 = 1000$, $R_3 = 1$ lead to nearly identical coordinates as in (c). $\mathcal{M}_0$ projects onto $\tilde{\boldsymbol{s}}_1$ in oblique coordinates and therefore decays along this direction, resulting in the spiral as shown.

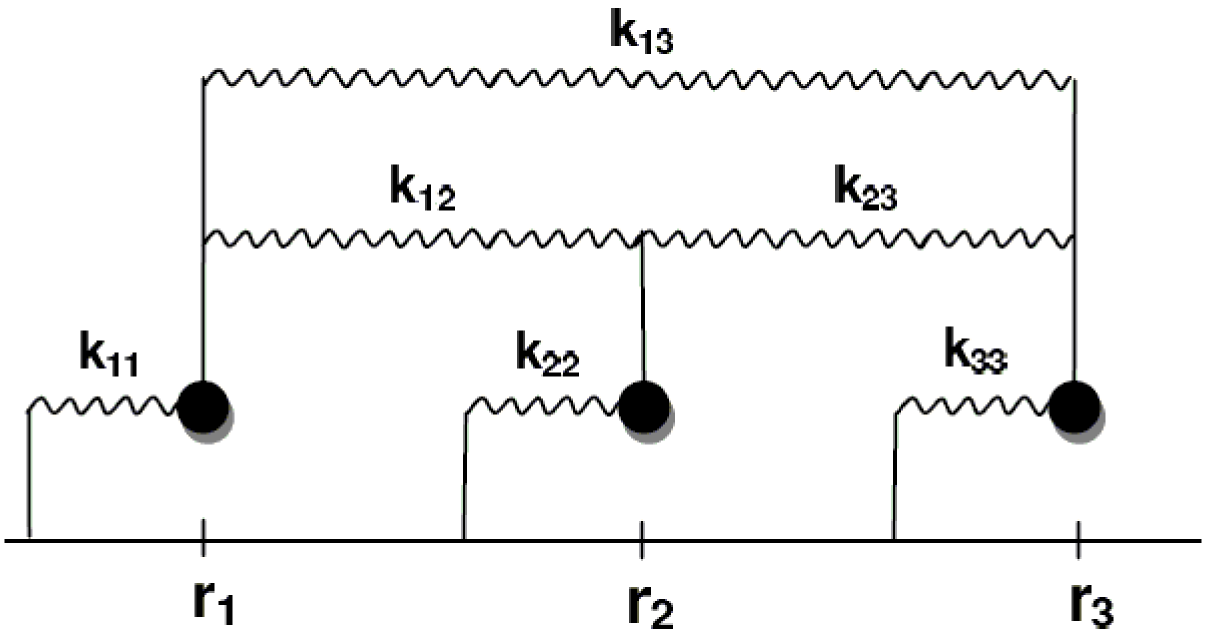

FIG. 4. The Bloch equation is shown in the text to model the displacements, from equilibrium positions $r_i = 0$, of a system of three unit masses coupled by springs of stiffness k_{ij}. One model identifies "velocity"-dependent damping terms. An alternative model is expressed as an ideal frictionless system that is, nonetheless, damped. Asymmetric couplings $k_{ij} \neq k_{ji}$ provide a dissipative mechanism in both models. The mechanical springs depicted in the figure are therefore only an analogy.